STUDIES OF BENZOIN AND STETTER REACTIONS USING MASS SPECTROMETRY

By

HAO ZENG

A thesis submitted to the

Graduate School-New Brunswick

Rutgers, The State University of New Jersey

in partial fulfillment of the requirements

For the degree of

Master of Science

Graduate Program in Chemistry and Chemical Biology

Written under the direction of

Jeehiun K. Lee

And approved by

_____

_____

_____

_____

New Brunswick, New Jersey

[October, 2014]

ABSTRACT OF THE THESIS

STUDIES OF BENZOIN AND STETTER REACTIONS USING MASS SPECTROMETRY

By HAO ZENG

Thesis Director:

Jeehiun K. Lee

This dissertation focuses on the study of benzoin condensation and the Setter reaction. Both experimental (mass spectrometry) and computational (Gaussian 09) methods were utilized.

A sulfonate charged tag thiazolium catalyst was synthesized and used to track the reaction process of benzoin consendation. Key intermediates corresponding to Breslow mechanism were isolated. Collision induced dissociation of the intermediates yielded fragments. The fragmention analysis was used to support structural assignments. In order to confirm the stablity of isomers, calculations were also conducted. Our results are consistent with a Breslow mechanism as opposed to dimer mechanism.

The acidity of two families of triazolium catalysts (morpholine-fused and pyrrolidine-fused triazolium) were studied in the gas phase. The experimental results were consistent with the calculations except for a pair of *trans* and *cis* fluorinated triazolium catalysts. Kinetic acidity issues were proposed to explain the discrepancies between calculations and experiments. This hypothesis was supported by conducting electrostatic potential surface calculation. The possible hypothesis of a bizarre reactivity and selectivity difference for *trans* and *cis* fluorinated catalysts were also proposed.

DEDICATION

To my parents, Xianlong Zeng and Min Sun, and to my fiancée, He Huang, for the endless love and support.

ACKNOWLEDGEMENTS

First and foremost, I would like to express my sincere gratitude to Dr. Jeehiun Katherine Lee, for her guidance and mentorship on my research projects these past three years.

I would also like to thank my committee members, Dr. Ralf Warmuth, Dr. Karsten Krogh-Jespersen for their time, attention and valuable advice with regards to my research projects.

I also want to thank Dr. Tomislav Rovis from Colorado State University for collaboration. In addition, I'd like to thank all my colleagues in the Lee group, especially Dr. Anna Zhachikina Michelson, Dr. Kai Wang, Dr. Mu Chen, Sisi Zhang, Yuan Tian, Yijie Niu, Landon Green for their generous help and support. I really enjoyed conducting research in the Lee group and feel like I gained new family members in my fellow coworkers.

I would like to thank my parents, Xianlong Zeng and Min Sun, for their endless love and support. They always believed in me and encourage me to chase my dream.

Last but not least, I want to thank my fiancée, He Huang. During these past three years she was always there to give me love and support. The time I spent with her was always wonderful and meaningful.

TABLE OF CONTENTS

LIST OF FIGURES

LIST OF TABLES

Chapter 1 Introduction

1.1 Overview

1.1.1 Benzoin condensation

The benzoin condensation reaction involves the dimerization of two aromatic aldehydes, particularly benzaldehydes. This reaction can be catalyzed by a nucleophile such as cyanide anion or *N*-heterocyclic carbene (NHC). A. J. Lapworth first proposed the mechanism for the cyanide catalyzed benzoin condensation in 1903.[1] The mechanism of the thiazolium-catalyzed benzoin condensation reaction was proposed by Ronald Breslow in 1958 (Figure 1) and was derived from the cyanide-catalyzed benzoin mechanism.[2]

Since Breslow's mechanistic proposal in 1958, various studies have been conducted to ascertain the mechanism of this reaction.[3-6] However, Lemal and coworkers claimed that the carbene dimer is actually catalytically active in the catalytic circle and proposed Lemal dimer mechanism (Figure 1.2).[7] In the 1980s, Castells and coworkers proposed an alternative dimer mechanism (Figure 1.3).[8] While the Breslow mechanism prevails, conflicting data supporting both the Breslow and the Castells mechanisms do exist.[3-6, 9-14]

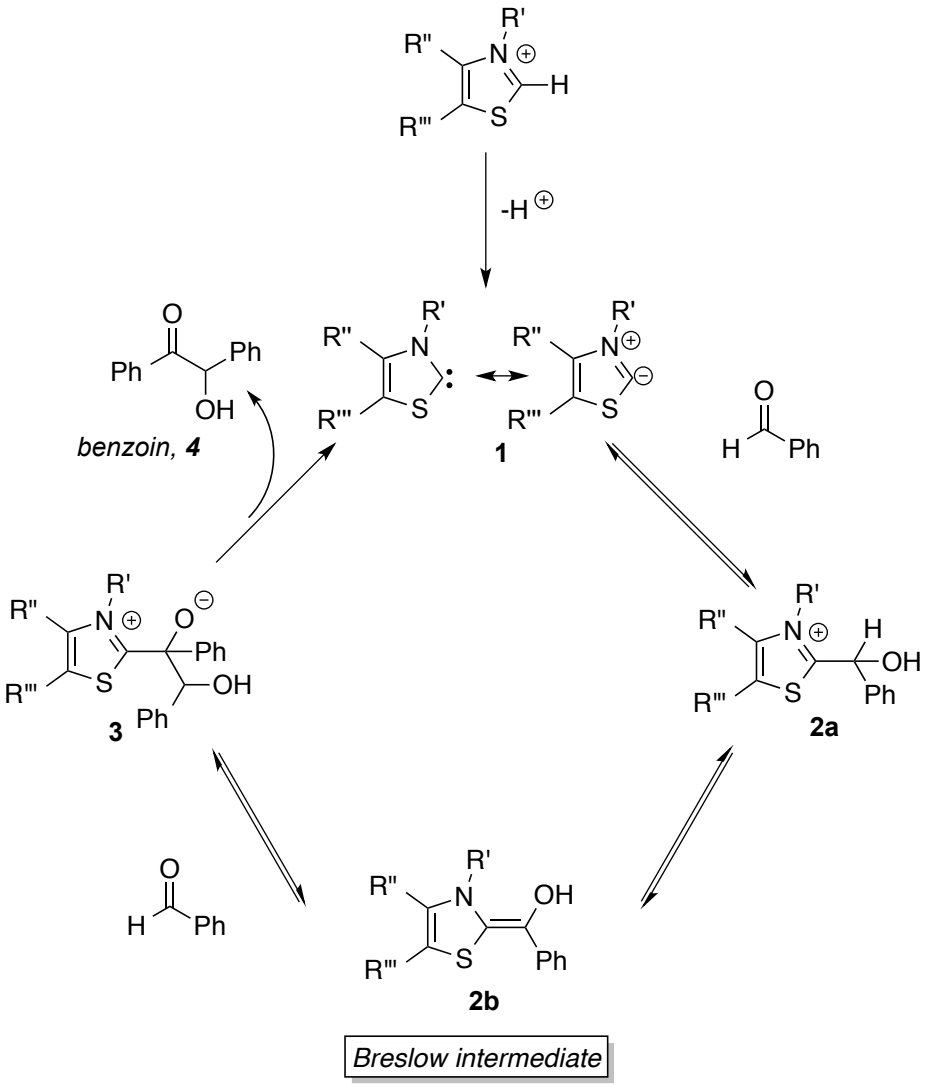

Figure 1. 1 Catalytic cycle of the benzoin condensation as proposed by Breslow.

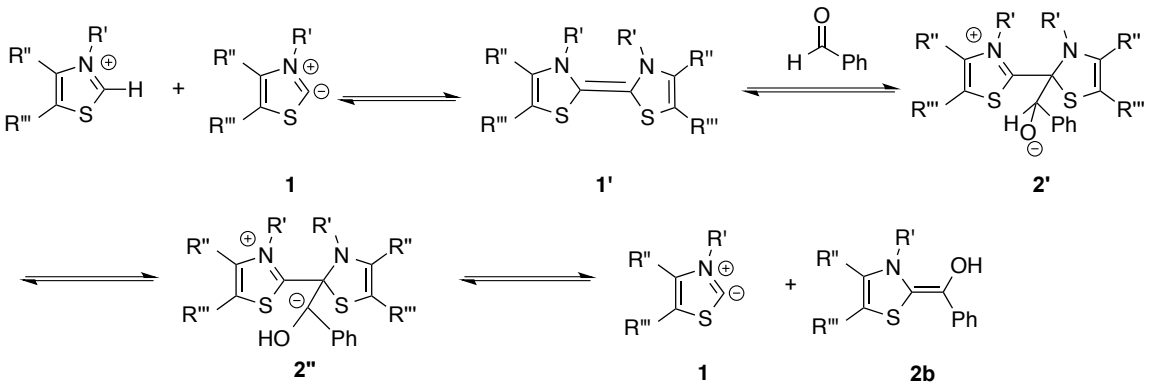

Figure 1. 2 Dimer mechanism proposed by Lemal.

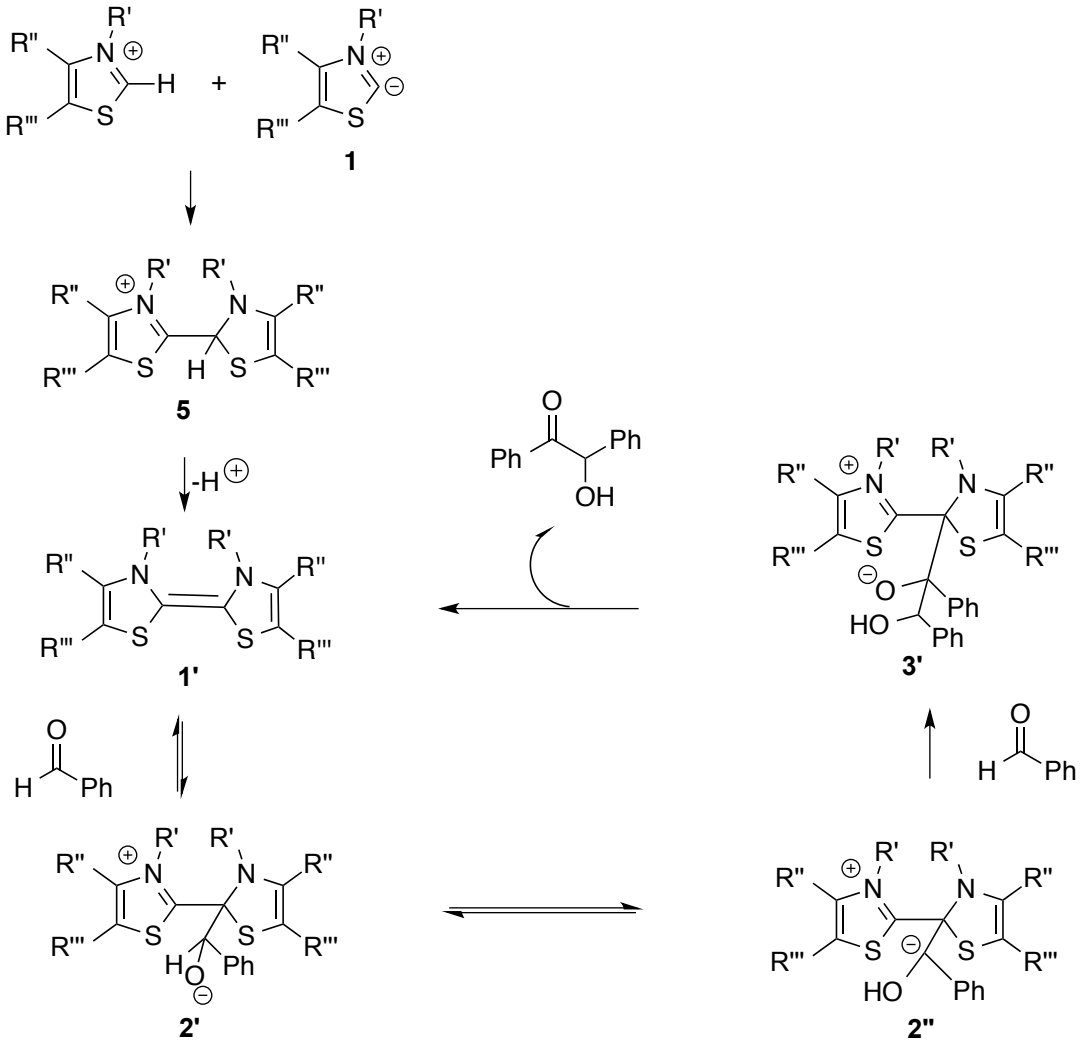

Figure 1. 3 Dimer mechanism proposed by Castells.

The enantioselective benzoin condensation reaction was developed by using chiral *N*-heterocyclic carbene (NHC), especially chiral thiazolium.[11, 15-18] Selected examples have been summarized in Table 1, and the catalysts shown in Figure 1.4.

Table 1. 1 Benzoin condensation catalyzed by thiazolium catalysts

Entry	Catalyst	Yield	ee	Reaction condition
1	I[1]	Up to 78%	Up to 52%	MeOH; Et_3N; 30 ^oC;24h. Benzaldehyde:Et_3N:catalyst=10:1:0.95
2	II[2]	Up to 20.6%	Up to 27%	MeOH; Et_3N; 0~30 ^oC ; 24h. Benzaldehyde:Et_3N:catalyst=10:1:1
3	III[3]	34%	20%	MeOH; Et_3N; 20 ^oC ; 18h. Benzaldehyde:Et_3N:catalyst=10:1.1:1
4	IV[3]	50%	20.5%	MeOH; Et_3N; 80 ^oC;3h. Benzaldehyde:Et_3N:catalyst=10:2.1
5	IV[4]	Up to 78%	Up to 51.5%	MeOH; Et_3N; 20~30 ^oC ; 24h. Benzaldehyde:Et_3N:catalyst=10:1:0.95
6	V[5]	Up to 82%	N.A.	THF; Et_3N; 60 ^oC; 22h. 2-chlorobenzaldehyde:Benzaldehyde:Et_3N:catalyst=10:10:2:1

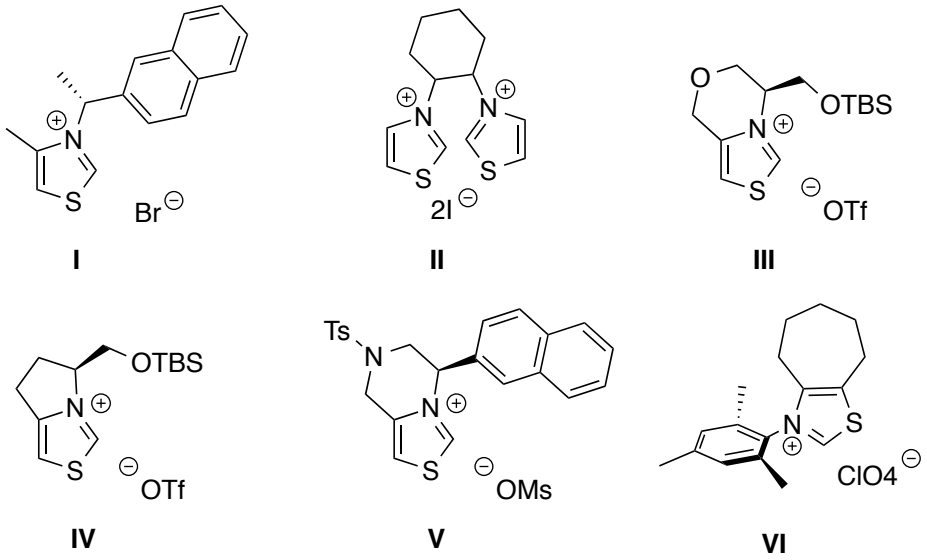

Figure 1. 4 Thiazolium catalyst in benzoin reaction

Elucidation of the reaction mechanism is necessary, as the understanding of the reaction will ultimately aid in the development of catalysts. One of the main issues with probing the reaction by mass spectrometry is the neutral charge state of the reactants. To track the reaction effectively, protonated forms of intermediates would be needed.[19-22] Alternatively, a charged and unreactive tag at the catalyst can be used to "fish" out intermediates.[23]. In this project, a sulfonate tagged thiazolium catalyst (Figure 1.5) was synthesized for the first time to track the process and the intermediates of the benzoin reaction.

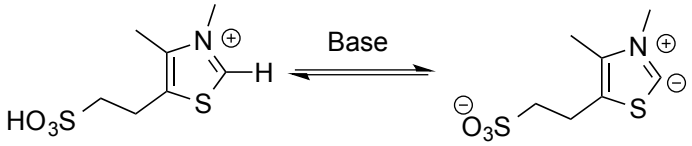

Figure 1. 5 Charge tagged thiazolium catalyst

1.1.2 Stetter reaction

The Stetter reaction is another example of *umpolung* chemistry, which involves a reversal in the polarity of an aldehyde group, rendering the carbon center nucleophilic rather than electrophilic.[24] The mechanism for the Stetter reaction was reported in 1973 by Dr. Hermann Stetter.[25] The Stetter reaction is very useful in synthetic chemistry, specifically in the formation of carbon-carbon bonds through a 1,4-addition using cyanide ions and thiazolium salts. Recently, triazolium salts have been found to be very effective in asymmetric Stetter reactions.

The first asymmetric intramolecular Stetter reaction was reported by Enders and coworkers in 1996 in low yields.[26] Later, Enders and coworker reported that intermolecular Stetter reaction catalyzed by triazolium salts can achieve very high yields

(up to 92%) with enantioselectivity (up to 78%).[27] In recent years, our collaborator Dr. Tomislav Rovis from Colorado State University made great contributions in developing asymmetric Stetter reactions.[28-36]

Dr. Rovis and coworkers began their study on Stetter reactions by using salicylaldehyde-derived tethered substrates (Figure 1.6). [28] An optimization study revealed that pre-catalyst **1** had the best selectivity, but gave only modest yields. Introduction of an electron-donating *para*-methoxy group on the azolium aryl ring resulted in catalyst **2**, which improved the yield and maintained the selectivity. Interestingly, the slightly electron-deficient *para*-chloro catalyst **3** yielded almost identical results as the parent phenyl pre-catalyst **1.** Moreover, pyrrolidine-fused salts **5** and **6** were also efficient pre-catalysts.

By using more electron-deficient catalysts, Dr. Rovis achieved cyclization onto trisubstituted alkene acceptors (Figure 1.7).[29] The use of pre-catalyst **3** provided the product in high enantiomeric excess (ee) but modest yields. A marked improvement in yield was observed with the very electron-deficient pentafluorophenyl-containing catalyst **6**. However, when cyclizing onto very electron-deficient alkenes (Figure 1.8), catalyst **9d** repeatedly provided low ee. While the use of the pyrrolidine catalyst **10a** provided high ee in this case.

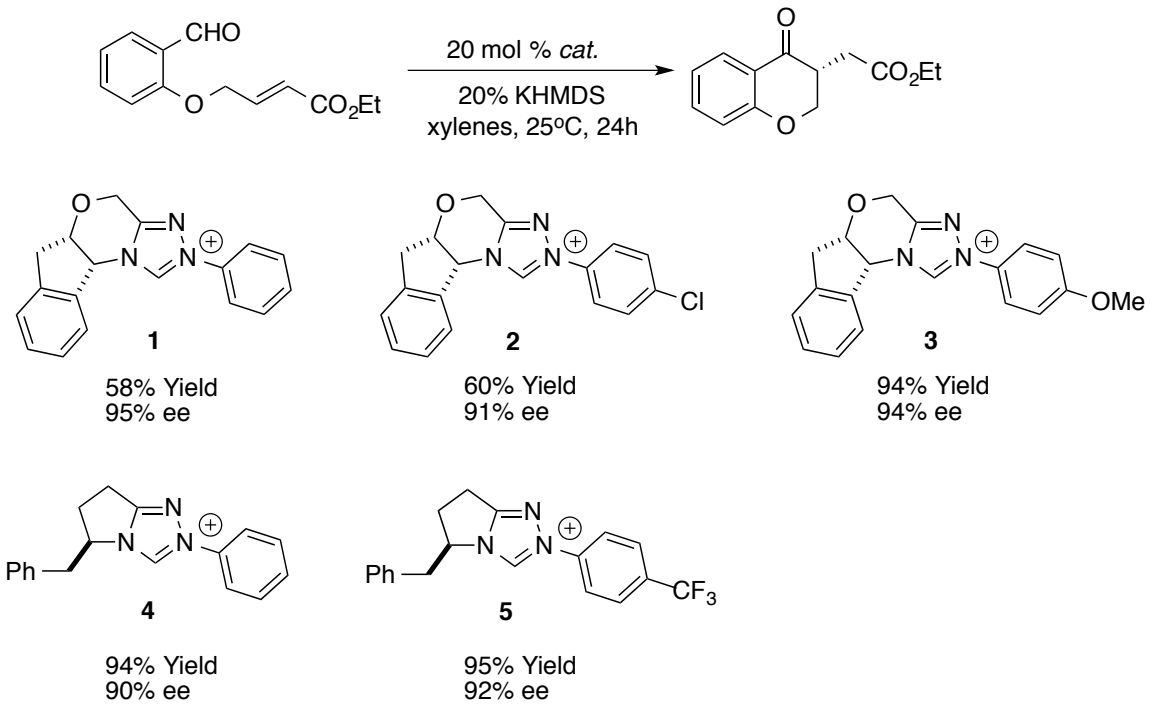

Figure 1. 6 Intramolecular Stetter reaction catalyzed by triazolium salts.

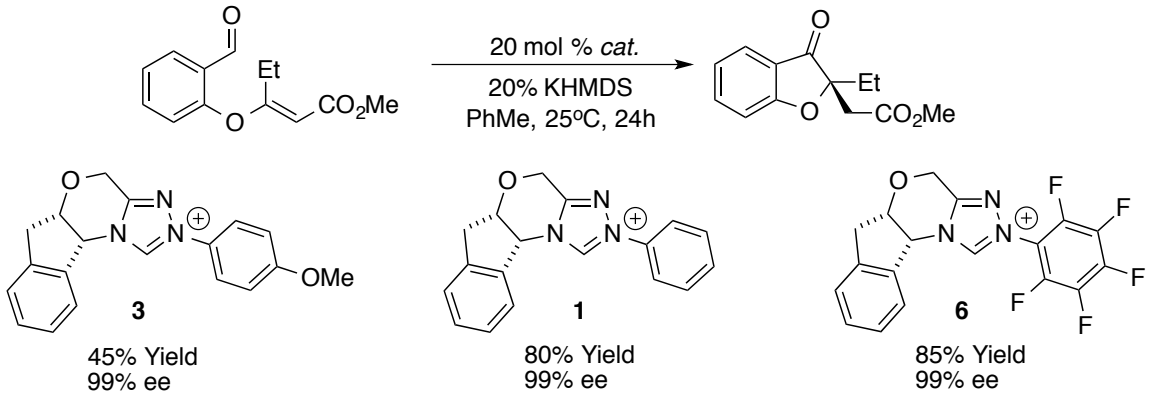

Figure 1. 7 Intramolecular Stetter reaction catalyzed by triazolium salts.

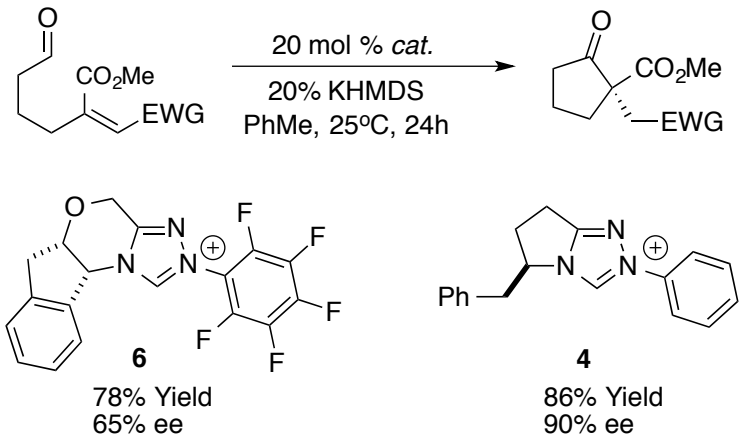

Figure 1. 8 Intramolecular Stetter reaction catalyzed by triazolium salts.

Aside from the asymmetric intramolecular Stetter reaction, Dr. Rovis reported his first asymmetric intermolecular Stetter reaction in 2008 (Figure 1.9).[30] In the pre-catalyst screen, catalyst **7** was the potential efficient catalyst compared with catalyst **4** and **6'**.

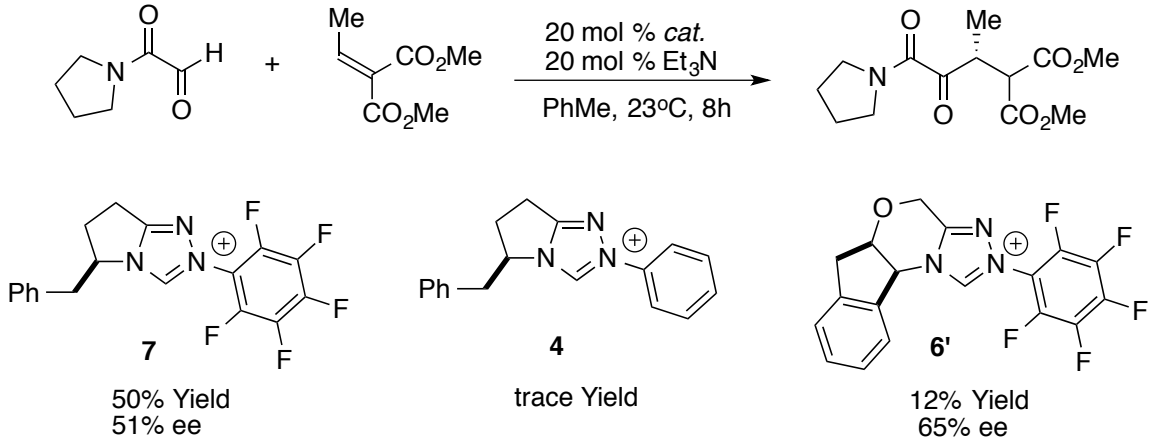

Figure 1. 9 Intermolecular Stetter reaction catalyzed by triazolium salts.

The second screen of substrates and reaction condition optimization achieved high yield and high ee (Figure 1.10).

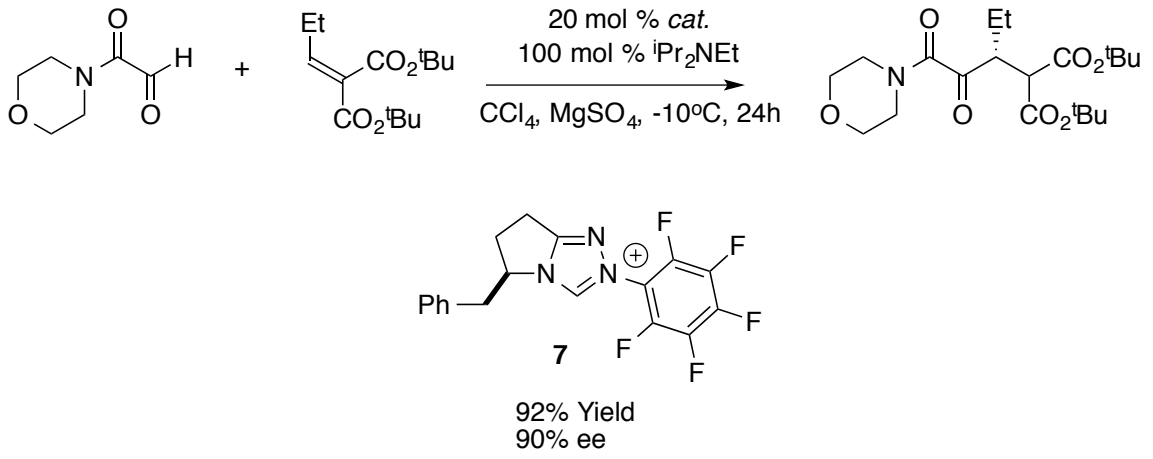

Figure 1. 10 Intermolecular Stetter reaction catalyzed by triazolium salts.

Dr. Rovis successfully developed two families of triazolium catalysts; the morpholine-fused triazolium salts and the pyrrolidine-fused triazolium salts. However, the fundamental properties of these catalysts have been little studied. Herein, we focused on calculating the proton affinities of these species and use our LCQ bracketing method to benchmark our calculation.

1.2 Instrumentation

1.2.1 Electrospray ionization (ESI)

The electrospray ionization technique was first developed by Masamichi Yamashita and John Fenn in 1984.[37] Since then, ESI has become a well-established and common method for the transfer of ions from solution to the gas phase at atmospheric pressure.[38] ESI ionizes samples at atmospheric pressure and belongs to atmospheric pressure ionization (API) sources. ESI is a considered a "soft ionization" method, since the process involves almost no fragmentation.

1.2.2 Modified Finnigan LCQ instrument for the bracketing method

We used Finnigan-LCQ ion trap mass spectrometer to measure the acidity and proton affinity of compounds (LCQ bracketing method). The ion trap mass spectrometer was first developed in the 1950s.[39]After decades of development, Hager developed the quadrupole ion trap mass spectrometer in 1998. Figure 1.11 is the Finnigan LCQ ion trap mass spectrometer used in this study. Ions are generated through electrospray ionization (ESI) and then focused using an electrostatic lensing system into the ion trap, which is filled with helium.

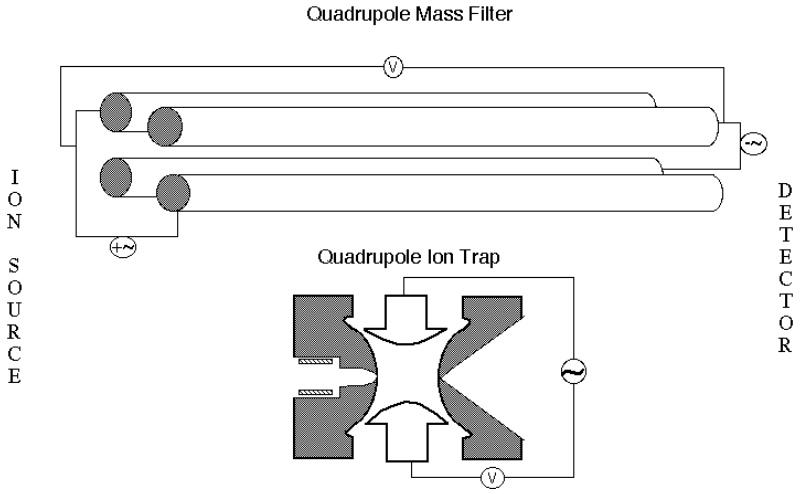

Figure 1. 11 Scheme of quadrupole ion trap

In order to introduce the neutral compounds in the form of vapors into the ion trap, the metal tubing carrying He gas was modified as shown in Figure 1.12. The neutral compound was added into a glass vial equipped with a Cajon connection. A cooling bath was used to control the temperature of the glass vial to maintain an appropriate constant pressure of the compound in the glass vial. A metering valve was used to adjust the amount of vapor carried by the He flow (from A) into the ion trap (D). A convectron

gauge was connected at position C in order to monitor the total pressure of the gas that goes into the ion trap.

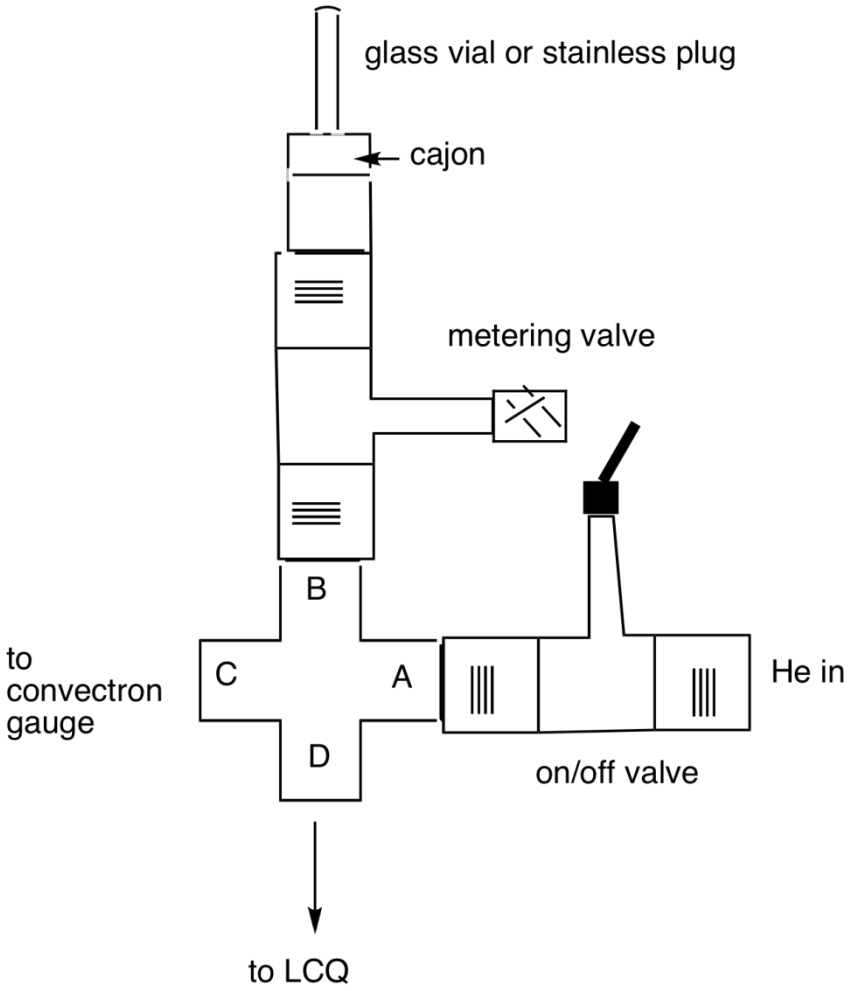

Figure 1. 12 Detailed scheme of neutral addition system for LCQ

1.3 Methodology

1.3.1 LCQ bracketing method

Bracketing experiments were conducted using a house-modified quadrupole ion trap mass spectrometer to measure the proton affinity and acidity of compounds of interest. The bracketing method uses bases or acids with known proton affinity or acidity, respectively, as references to react with unknown compounds.[40-41] By monitoring the proton transfer reactions between the unknown compounds and the references, proton affinities (PA) and acidities of the unknowns were determined. For example, compounds that were deprotonated by the reference base have a lower PA than the reference. On the other hand, if the reference base fails to deprotonate the unknown compound, the PA of the unknown should be higher than the PA of the reference base. A series of reference bases and acids can be utilized to narrow down the PA and acidity range of the unknown.

1.3.2 Computational method

All calculations were conducted using density functional theory at B3LYP/6-31+G(d) as implemented in Gaussian09. All of the geometries were fully optimized and the frequencies were calculated in such a way that optimized structures didn't have negative frequencies.[42-46] All the values reported are at 298 K. No scaling factor was applied.

Chapter 2 Probing the mechanism of benzoin condensation by using charge-tagged thiazolium catalyst

2.1 Introduction

Benzoin condensation, which involves the dimerization of two benzaldehyde, has been intensively studied ever since 1903. In 1943, Ukai and coworkers reported that thiamin (Figure 2.1) and related thiazolium salts were able to catalyze the benzoin reaction in the presence of a mild base.[47] Breslow proposed an analogous mechanism to the one proposed by Lapworth a decade later using thiazolium salts.[2] Breslow's mechanism (Figure 1.1) features the formation of thiazolium C2 ylide - the thiazolylidene **1**. Nucleophilic attack of the aldehyde by NHC or a zwitterion yields a tetrahedral intermediate, which undergoes proton transfer to give an acyl anion equivalent commonly called the "Breslow intermediate". This acylation reagent demonstrates the *umpolung* reactivity (the aldehyde becomes nucleophilic instead of electrophilic) and reacts with another molecule of benzaldehyde to give a new carbon-carbon bond. A second proton transfer forms tetrahedral intermediate **3**, allowing for the elimination of the benzoin and the original catalyst is regenerated.

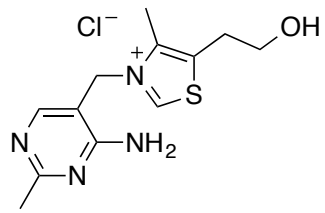

Figure 2. 1 The structure of thiamin

The Breslow mechanism has been widely accepted with many evidences in support of it. Jordan and coworkers successfully isolated a 2-(α-hydroxybenzyl)-3,4-dimethylthiazolium salt (analogue of **2a,** Figure 1.1) that was found not to decompose to benzaldehyde and 3,4-dimethylthiazolium ion, rather it was able to proceed to benzoin and thiazolylidene **1** formation when treated with excess benzaldehyde.[3] Krampitz and co-workers obtained similar results.[48] Berkessel and coworkers isolated the Breslow intermediate in its keto form and Rovis derived a Breslow intermediate analogue from chiral triazolylidene carbenes.[49] However, the isolation and characterization of the Breslow intermediate itself was not realized until 2012, when Berkessel and coworkers isolated the imidazolium based Breslow intermediate and characterized it spectroscopically.[6] These are all strong evidences of the Breslow mechanism.

The Breslow mechanism was challenged by Lemal and co-workers, they proposed an alternative mechanism for benzoin condensation-the Lemal mechanism (Figure 1.2) in which the bis(thiazolin-2-ylidenes) **1'** acts as a nucleophile and reacts with a aldehyde to form **2'**.[7] After the proton transfer and a subsequent fragmentation, an intermediate that corresponds to the Breslow enamine (**2b**) and zwitterion **1** is generated. Then the reaction is believed to proceed through the Breslow mechanism.

In the 1980s, Castells and co-workers proposed a new dimer mechanism for benzoin condensation.[8] The new dimer mechanism was different from the Lemal mechanism in that **2"** would not undergo dissociation but pick up another benzaldehyde to form **3'** (Figure 1.3). In this mechanism, the carbene dimer is the real catalyst rather than carbene monomer.

These three proposed mechanisms for benzoin condensation have been intensively discussed in the past years. Evidences in support of and against the dimer mechanisms do exist.[3-14] Nevertheless, the Breslow mechanism is well accepted.

Understanding the mechanism of a reaction is pivotal, as it could guide us to the design and modification of catalysts to achieve high chemical transformations. NMR is an effective way to track reactions and provides valuable information regarding the reaction mechanism. In recent years, electrospray ionization (ESI) coupled with mass spectrometry (MS) has become a potent and reliable method to track the progress of organic reactions.[19-22] ESI is a “soft” ionization method, making it possible to transfer ions formed in the solution directly into the gas phase and "fish” out the positively or negatively charged ions. Some of the intermediates were trapped in this way. By using the tandem MS/MS technique, the selected ions were subjected to collision induced dissociation (CID), which may provide direct information about the structure of the investigated ions. Due to the high sensitivity of this method, the structure identification of short-lived or low concentration intermediates could be achieved.

Because of the importance of *umpolung* reactions, we took the advantage of ESI-MS to track the progress of such reactions, starting with the well-known benzoin condensation. In order to monitor the reaction by mass spectrometry, the relevant intermediates must be charged. However, the carbene species or zwitterion presents in benzoin condensation, which is undetectable by mass spectrometry. To address this issue, a charged tag was introduced on the catalyst so that all steps involving the catalyst could be detected. This technique has achieved recognition over the years. We successfully

synthesized a thiazolium catalyst with a sulfonate charge tag and used it to study the benzoin condensation.

2.2 Experimental

2.2.1 Synthesis details

A solution mixture of 1,5-dimethyl-4-(hydroxyethyl) thiazolium iodide (2.5 mmol, 700 mg), methylsulfonyl chloride (3 mmol, 0.25 ml) and triethylamine (5 mmol, 0.35 ml) in CH_3CN (20 ml) was stirred at 0^oC for 2 hours, under the protection of argon. After rotary evaporation, the crude product was dissolved in ethanol (25 ml). Potassium thioacetate (3 mmol, 343 mg) was added dropwise and the mixture was allowed to reflux for 72 hrs. The product mixture was rotary evaporated to dryness, then the resultant crude solid was dissolved in formic acid (5 ml). Performic acid was generated by stirring hydrogen peroxide (14 mmol, 1.8 ml) and formic acid (30 mmol, 1.4 ml) at room temperature for one hour. The performic acid solution was cooled to 0^oC and added to the reaction mixture. The mixture was left stirring for 48 hours. Excess solvent was removed by rotary evaporation and the final crude product was purified by HPLC. ^1H NMR (300 MHz, DMSO-d6) δ 9.90 (s, H), 4.05 (s, 3H), 3.14-3.19 (t, J = 7.1 Hz, 2H), 2.70-2.75 (t, J = 7.0 Hz, 2H), 2.41 (s, 3H).)

2.2.2 Benzoin condensation reaction condition

The synthesized thiazolium was dissolved in methanol to make a 0.1M solution.

Argon was bubbled in for five minutes to expel oxygen. 10 equivalents of benzaldehyde and 2.5 equivalents of triethylamine were added to the reaction solution. The reaction was stirred at room temperature and tracked over time. To track the reaction by mass spectrometry, an aliquot from the reaction mixture was diluted to make a 100 uM (in thiazolium) solution, which was then injected into the ESI source.

An electrospray needle voltage of ~4 kV and flow rate of 25 μL/min was used to volatilize the reaction mixture. Full scan spectra are an average of forty scans. For MS/MS, the ions were isolated and activated for 30 ms, at varying (5-30%) collision energies.

2.2.3 Calculation method

Calculations were conducted at B3LYP/6-31+G(d) using Gaussian09; the geometries were fully optimized and frequencies were calculated.[42-46] All the values reported are at 298 K. No scaling factor was applied. For the solvation calculations, the integral equation formalism variant of the polarizable continuum model, using radii and non-electrostatic terms for Truhlar and coworkers' SMD solvation model, was utilized.[50-52]

2.3 Results and discussion

2.3.1 Charge-tagged thiazolium catalyst

The synthesis of charge-tagged thiazolium catalyst is shown in Figure 2.2. A commercially available thiazolium with a hydroxyl side chain was reacted with

methanesulfonyl chloride to yield the sulfonic ester. Further reaction with potassium thioacetate yielded the thioester. Finally, oxidation by performic acid yielded the sulfonate-tagged thiazolium product.

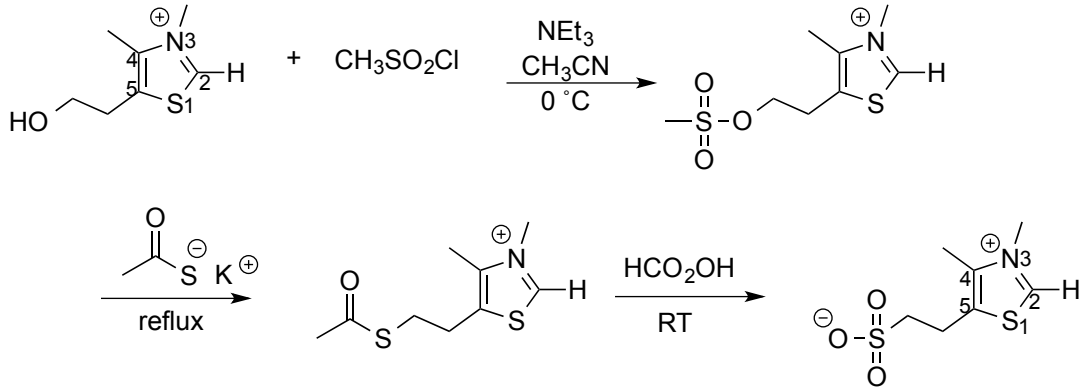

Figure 2. 2 Synthesis of charge-tagged thiazolium.

2.3.2 Benzoin condensation reaction by MS

The thiazolium catalyst was deprotonated by triethylamine and reacted with benzaldehyde. The reaction was monitored by mass spectrometry. The first spectrum was taken after 5 minutes of the reaction time and tracked every 20 minutes afterwards for a total of 185 minutes. The spectrum after 5 minutes of the reaction time is shown in Figure 2.3. The resulting ESI(-)-MS revealed predominant and abundant ions of *m/z* 220, *m/z* 326 and *m/z* 441, which corresponds to the deprotonated catalyst **1,** the first key intermediate derived from the addition of one benzaldehyde **2** and thiazolylidene-thiazolium dimer **5**. We also observed *m/z* 121, which is deprotonated benzoic acid and resulted from oxidation of benzaldehyde. As the reaction time proceeds, the benzoate ion (*m/z* 121) and oxidized catalyst (*m/z* 236) become the dominant peaks. However, we didn't see *m/z* 432 (**3**), which is the second key intermediate resulting from the catalyst

plus two benzaldehyde and *m/z* 211, corresponding to the deprotonated benzoin product.

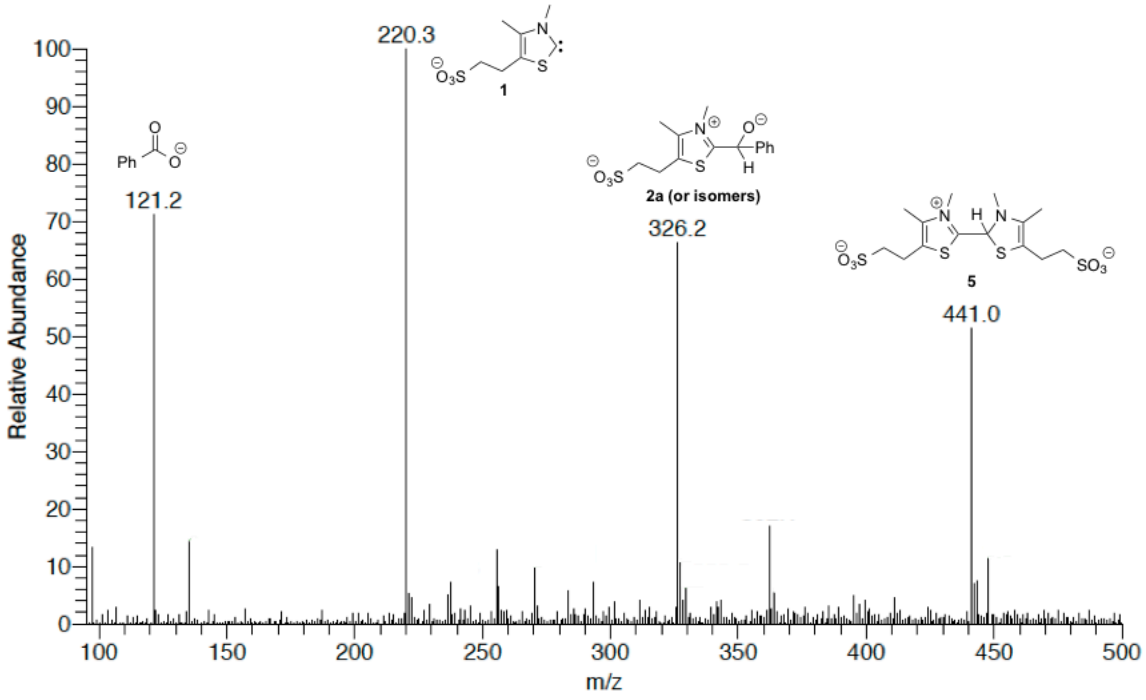

Figure 2. 3 Mass spectrum of reaction mixture after 5 minutes.

2.3.3 Intermediates interpretation by MS/MS and calculation

To confirm the possible structures of the intermediates in the reaction, we isolated these ions and subjected them to collision-induced dissociation (CID). The MS/MS spectrum of *m/z* 220 is shown in Figure 2.4. Upon CID, the thiazolium catalyst **1** will lose its sulfonate tag ion with *m/z* 81. Because of the possible dimer mechanism, *m/z* 220 could also be the dimer **1'** (Figure 2.5). However, if *m/z* 220 is dimer **1'**, we expected it to loss only one of the sulfonate charged tags with a final *m/z* of 359. We didn't observe the peak corresponding to *m/z* 359, thus we think *m/z* 220 is the monomer **1** instead of dimer **1'**. The ion *m/z* 441 corresponds to the precursor of dimer **1'**. The MS/MS spectrum of *m/z* 441 (figure 2.6) shows that there is only one daughter ion with *m/z* 220, which is the thiazolium carbene or zwitterion.

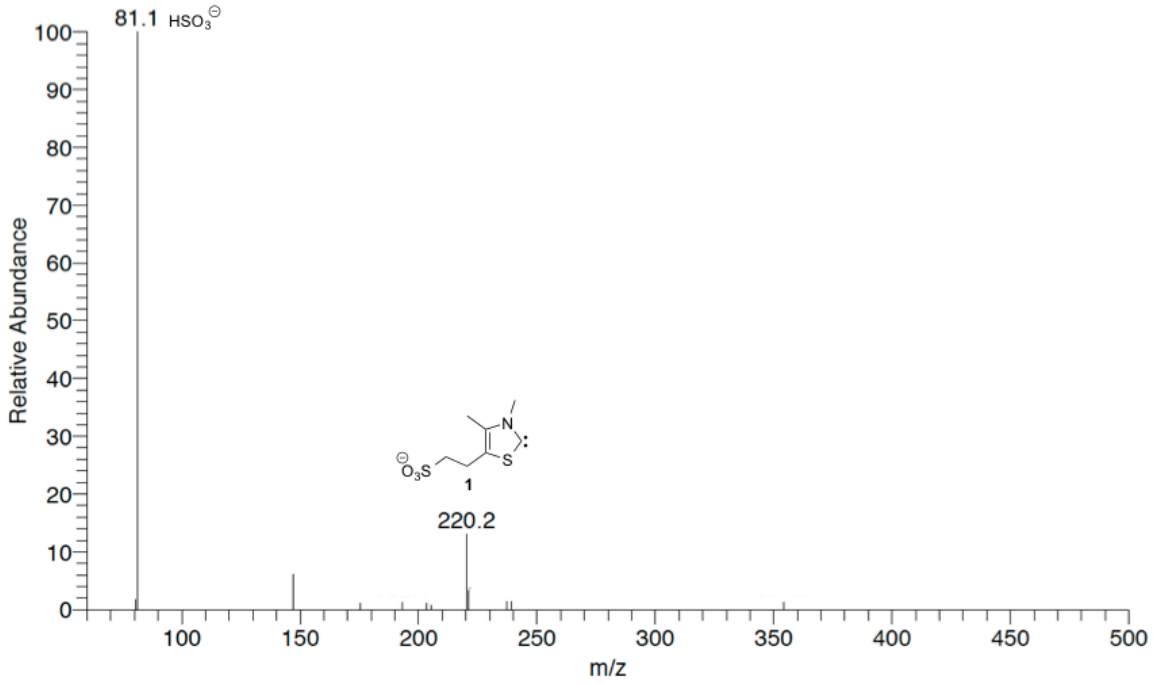

Figure 2. 4 MS/MS spectrum of *m/z* 220.

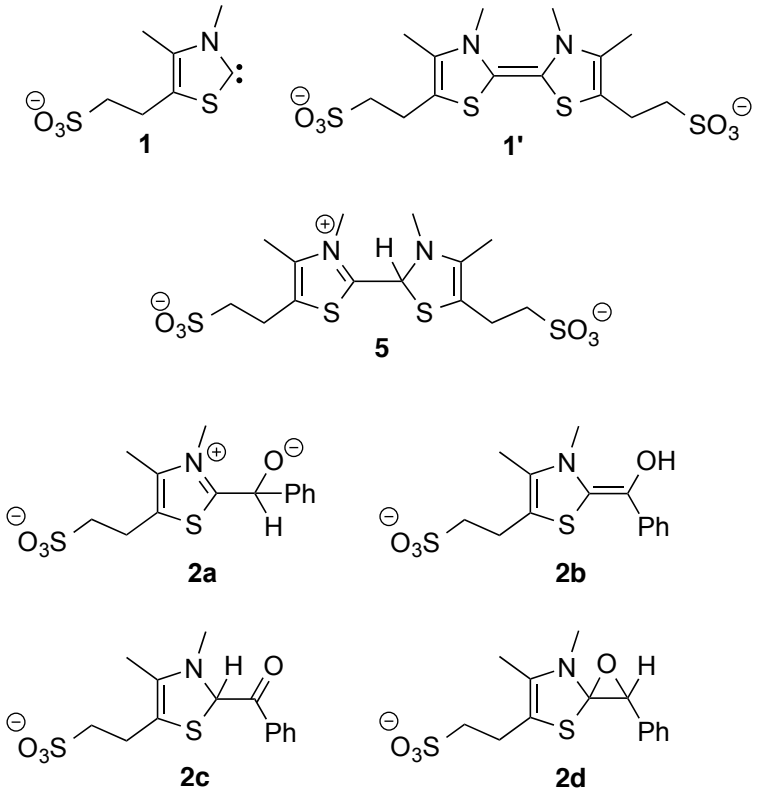

Figure 2. 5 Possible structures of observed *m/z*.

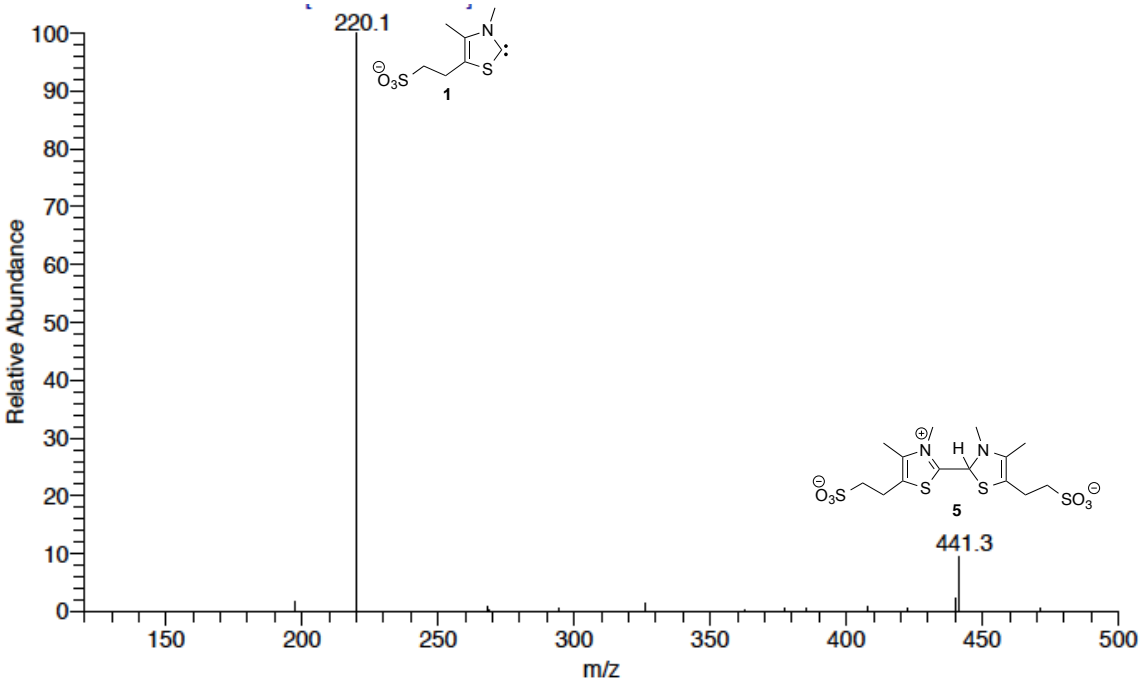

Figure 2. 6 MS/MS spectrum of *m/z* 441.

There are many possibilities for the structure assignment of *m/z* 326. It could be the tetrahedral intermediate **2a** or Breslow intermediate **2b**. Both of these two intermediates have the same *m/z* and are present in the Breslow mechanism. The MS/MS of *m/z* 326 is shown in Figure 2.7. The dominant daughter ion *m/z* 311 could result from the loss of methyl radical from *m/z* 326 (only fragments correspond to Breslow intermediate is shown). The parent ion could kick out benzaldehyde and yield thiazolium **1**. Interestingly, the water loss pathway is also observed, as the daughter ion *m/z* 308 is present. Other possible structures for *m/z* 326 could be the ketone **2c** and epoxide **2d** (Figure 2.5), which have been reported before. Since our fragmentation analysis cannot differentiate among these structures, we did calculations to explore the structure further. The relative stabilities of these ions (*m/z* 326) is shown in Figure 2.8. It turns out that ketone **2c** is 6.9 kcal/mol more stable than the Breslow intermediate and 14 kcal/mol

more stable than tetrahedral intermediate **2a**. Also, the epoxide structure **2d** is 19.4 kcal/mol less stable than the ketone **2c**. This may explain why the Breslow intermediate is so difficult to isolate and why the ketone **2c** could be isolated.

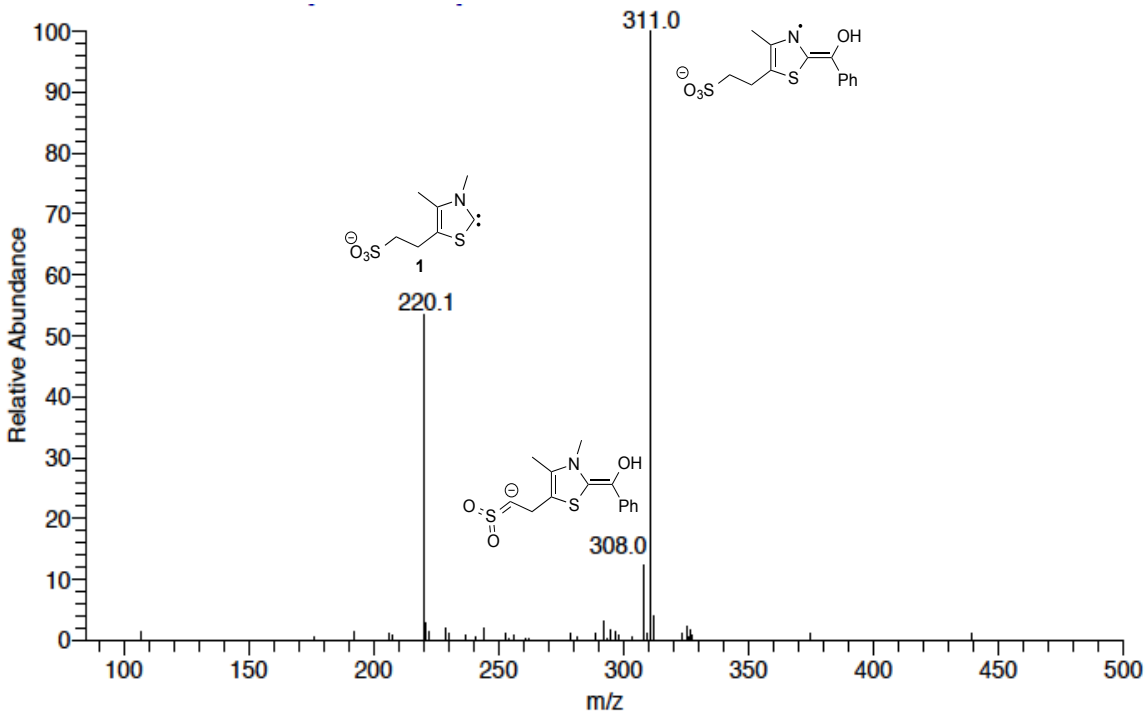

Figure 2. 7 MS/MS spectrum of *m/z* 326.

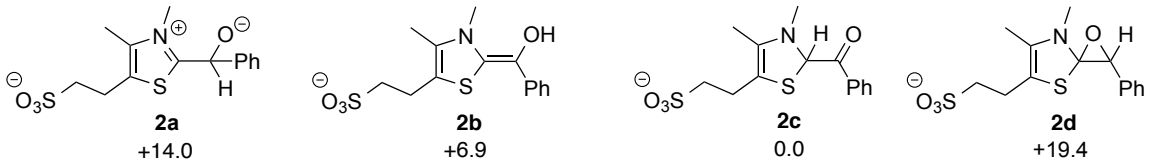

Figure 2. 8 Relative stabilities for the possible structures for 2, *m/z* 326 (ΔH at 298K, B3LYP/6-31+G(d)).

2.3.4 Breslow mechanism *vs* dimer mechanism

In this study, we observed *m/z* 220, the thiazolium carbene **1** or zwitterion. We also saw *m/z* 326, which could be the tetrahedral intermediate **2a** or the Breslow intermediate **2b**. While our calculation shows that ketone **2c** is the most stable intermediate, we cannot

rule out the possibility that **2a** and **2b** were present, since they may be reactive and undetectable by mass spectrometry. In our reaction condition, we didn't observe m/z 432, the second intermediate **3** presumably because intermediate **3** is short-lived, once it is formed, it will release the benzoin product **4** immediately. We are not surprised that we didn't see *m/z* 211 (deprotonated benzoin, **4**) since ketones have pK_a values of 19-20 and triethylamine is not a strong enough base to deprotonate the benzoin product and make it a charged species.

For the dimer mechanism, we saw *m/z* 441 (Figure 2.9), which is the precursor of the dimer catalyst **1'**. We have no evidence to support the existence of **1'**, so we have concluded that *m/z* 441 is not catalytically active. Also, *m/z* 326 might be **3'** in the dimer mechanism; however, the fragmentation of *m/z* 326 shows no support for this structure. There is one unique ion m/z 273 in the dimer mechanism, which is the dimer catalyst plus one benzaldehyde. We didn't observe it. Based on these facts, we think dimer mechanism is not practical under our condition, though we cannot completely deny the possibility of a dimer mechanism, since *m/z* 273 could be very short-lived and therefore undetectable by mass spectrometry.

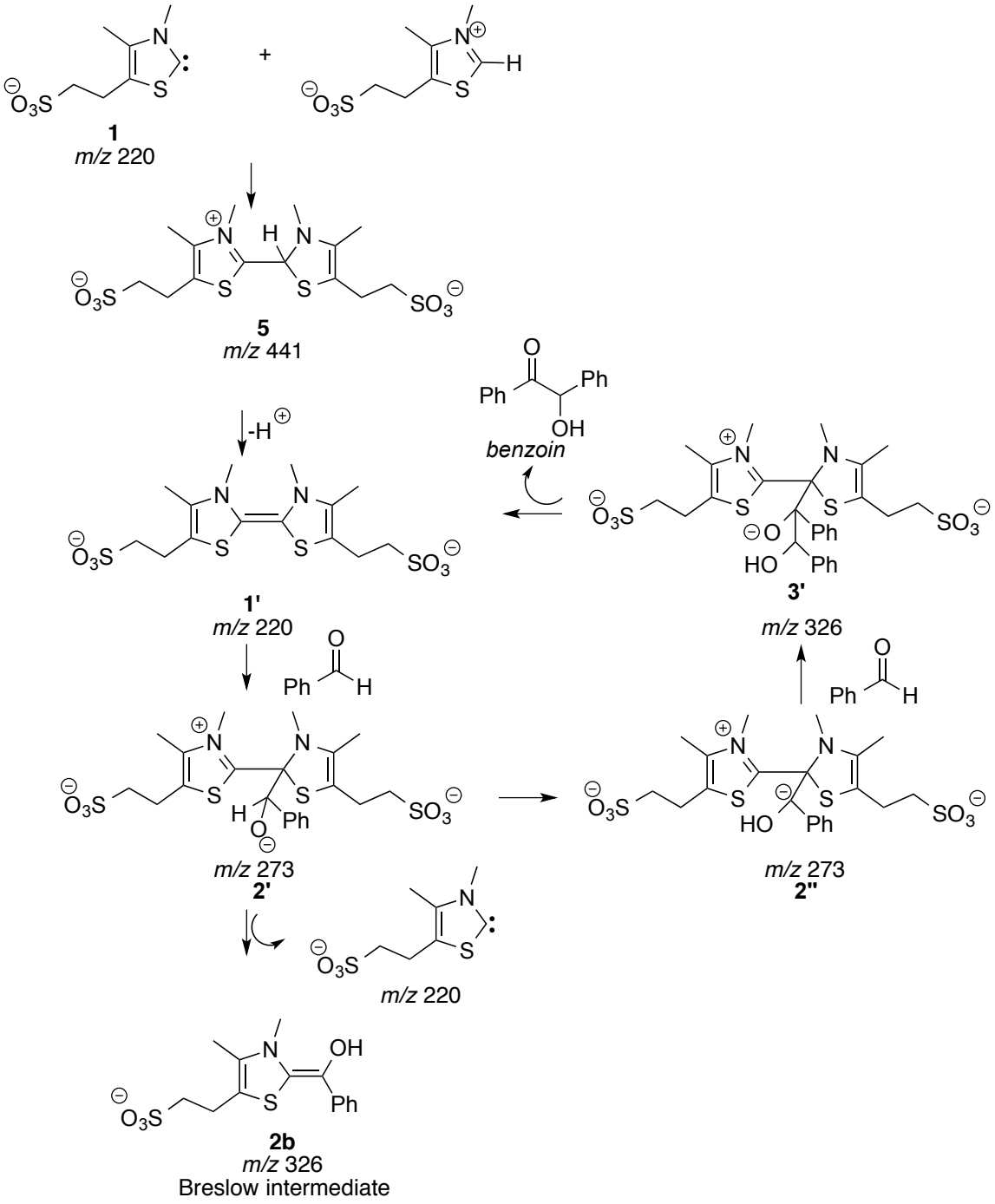

Figure 2. 9 Dimer mechanism for benzoin condensation.

2.3.5 Thiazolium catalyst with *vs* without charged tag

Given that we used charge-tagged catalyst in the reaction, it's good to know how the charge tag will affect the reaction. We calculated the proton affinity of the thiazolylidene

1 and its neutral counterpart (**1H**, Figure 2.10). Gas phase calculations reveal that the negatively charged sulfonate tag significantly increases the proton affinity at the reactive carbene center, **1** which is 71 kcal/mol more basic than **1H**. However, this proton affinity difference is significantly diminished when solvation is considered (calculations in a water dielectric). In water, **1H** is calculated to be slightly more basic than **1**, with 3 kcal/mol difference. Therefore, our charged catalyst may not make a difference in catalytic reactivity compared with the neutral counterpart.

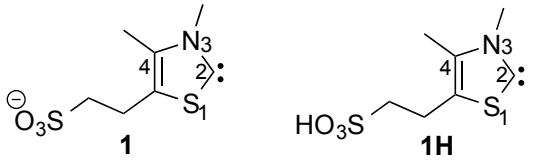

Figure 2. 10 Charged catalyst and its neutral counterpart.

2.3.6 Charge-tagged imidazolium catalyst in benzoin condensation.

As a comparison of thiazolium charge-tagged catalyst, we also explored the potential usage of imidazolium charge-tagged catalyst in probing the benzoin condensation (Figure 2.11). Preliminary results showed that charge-tagged imidazolium catalyst can catalyze the benzoin reaction but with slower rate compared with thiazolium. Further study of imidazolium charge-tagged catalyst is still ongoing in our group.

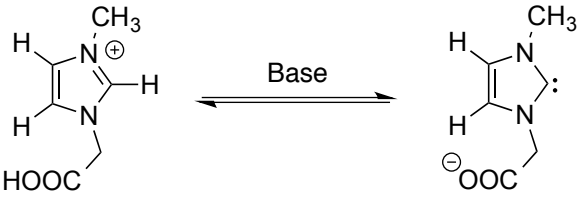

Figure 2. 11 Charge tagged imidazolium catalyst

2.4 Conclusion

We have designed a novel thiazolium catalyst with a negatively charged tag, and used it for probing the benzoin condensation. Intermediates corresponding to the Breslow mechanism were “fished” out and characterized. Under our reaction condition, the Breslow mechanism is dominant and a dimer mechanism is unlikely.

Chapter 3 Chiral triazolium catalysts in Stetter reaction

3.1 Introduction

Stetter reaction is another *umpolung* reaction, which involves an aldehyde and Michael acceptor (α, β-unsaturated ketone, ester or nitrile) as reaction substrates to give 1,4-diketones, 4-ketoesters, or 4-ketonitriles.[25] The proposed mechanism of the Stetter reaction (Figure 3.1) is based on the triazolylidene-catalyzed benzoin condensation mechanism of Breslow. The catalytic cycle starts with the carbene or zwitterion **1**, formed *in situ* from the azolium salt. The nucleophilic attack of carbene **1** to the aldehyde formes tetrahedral intermediate **2a**. First proton transfer occurs to generate the acyl anion equivalent ("Breslow intermediate") **2b**. This then adds to the Michael acceptor to form **3**. Proton transfer yields **4**, which then collapses to form the Stetter product and release of the catalyst.

The intramolecular Stetter reaction has drawn much more attention than intermolecular Stetter reactions. In 1995, Ciganek published a paper on intramolecular Stetter reaction by using thiazolium catalyst (Figure 3.2).[54] Ciganek's reactions are interesting because later scientists use his reactions to test and benchmark the efficiency and selectivity of catalysts. In 1996, Enders conducted the first asymmetric Stetter reaction using triazolium catalyst.[26] Since 2002, Rovis and coworkers disclosed several publications and are considered expert scientist at the forefront of this area.[28-36] They mainly applied two scaffolds in designing the triazolium catalysts (Figure 3.3): the morpholine-fused triazolium salts **I** and the pyrrolidine-fused triazolium salts **II**.[55] Their

ideas originated from Leeper and Rawal who first proposed to use these "locked backbones" for asymmetric benzoin condensation. [16-17]

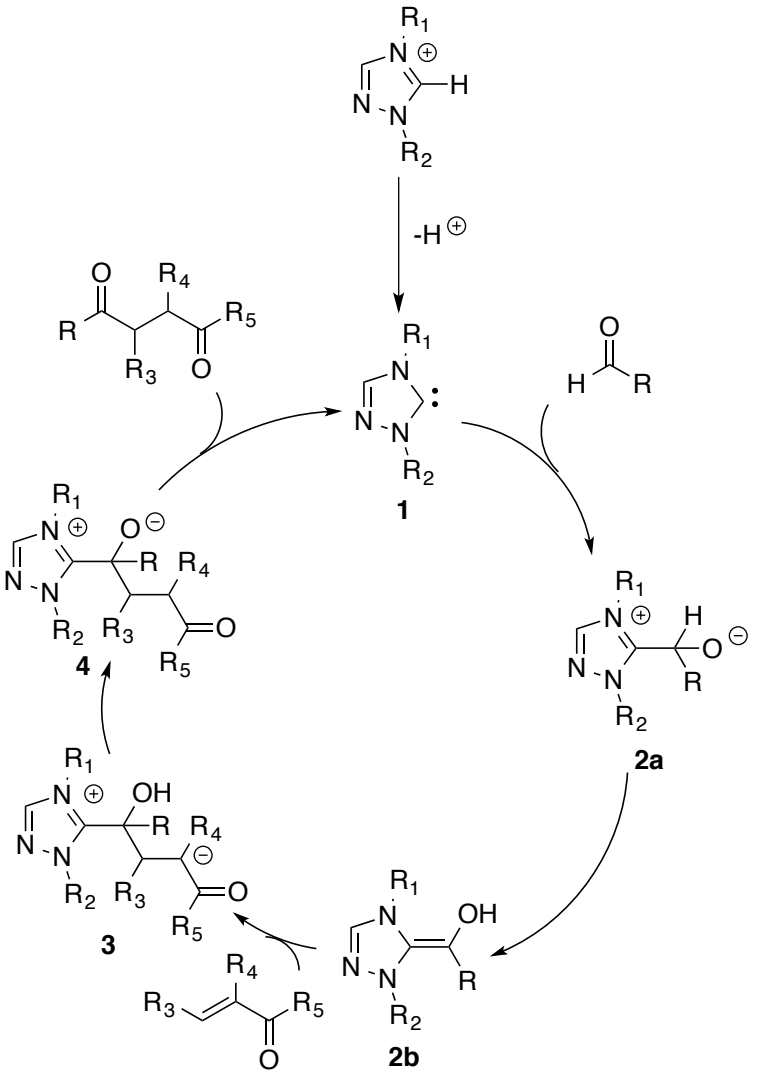

Figure 3. 1 Proposed mechanism for Stetter reaction by triazolium.

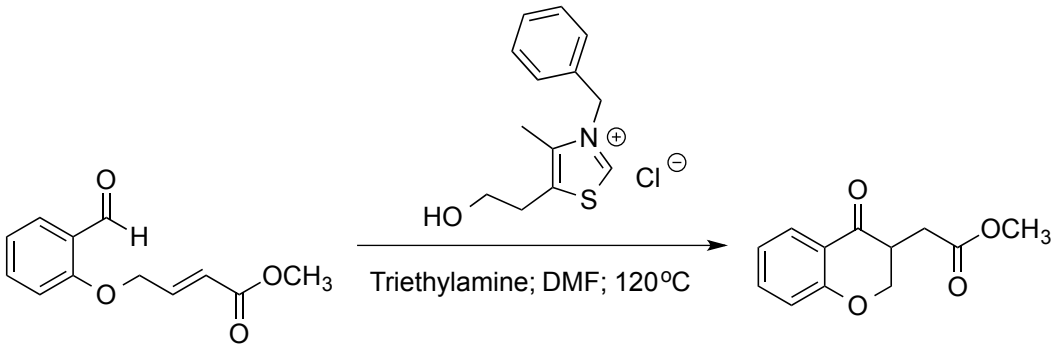

Figure 3. 2 Intramolecular Stetter reaction catalyzed by thiazolium.

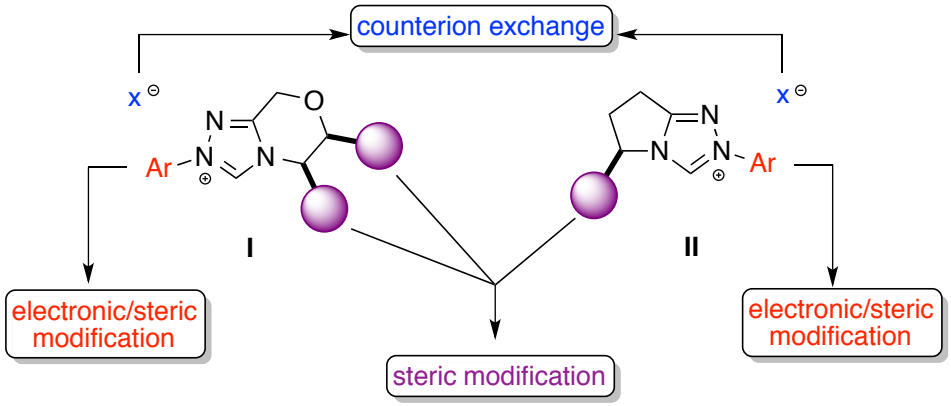

Figure 3. 3 Chiral bicyclic triazolium scaffolds

Despite the success of these two families of catalysts on Stetter reaction, very few fundamental reactivity studies have been conducted. Understanding the fundamental properties will aid in the continued development, design, application and mechanistic understanding of these catalysts. In our lab, we used two methods to study the proton affinity of these carbene catalysts, one is the calculation method and the other one is the bracketing method, which can benchmark our calculation results.

3.2 Experimental.

3.2.1 Bracketing method

Bracketing experiments were conducted using a house-modified quadrupole ion trap mass spectrometer as described in chapter 1. Protonated carbene ions (triazolium) were generated in the gas phase by electrospray ionization (ESI) with a flow rate of 25 μL/min. The trizolium salts were dissolved in methanol to produce a 10^{-4} M solution. The capillary temperature was 150 °C. Neutral reference bases were added with the helium gas flow. The protonated carbene ions were allowed to react with neutral reference bases for 0.03-1000 ms. The occurrence of proton transfer was regarded as evidence that the reaction was exothermic ("+" in Tables); otherwise the reaction was regarded as endothermic ("–" in Tables). The typical electrospray needle voltage was ~2.5 kV. A total of 10 scans were collected.

3.2.2 Calculation method

Calculations were conducted at B3LYP/6-31+G(d) using Gaussian09; the geometries were fully optimized and frequencies were calculated.[42-46] All the values reported are at 298 K. No scaling factor was applied. For the solvation calculations, the CPCM model was utilized. GaussView 5.0 was used to generate the electrostatic potential maps of the protonated carbenes based on their optimized structures in the gas phase. Density isovalues for the surfaces were set to 0.0004. The color range for the surfaces was set to -

0.19 to +0.19.

3.3 Results and discussion

3.3.1 Calculation results

The acidity of the protonated morpholine-fused triazolium catalyst is shown in Figure 3.4. According to the calculation, fluorine-modified triazolium salts are more acidic than nonfluorinated analogues as expected. Bulky substituents decrease the acidity of the triazolium salt. *Cis*-fluoro and *trans*-fluoro triazolium salts have comparable acidities.

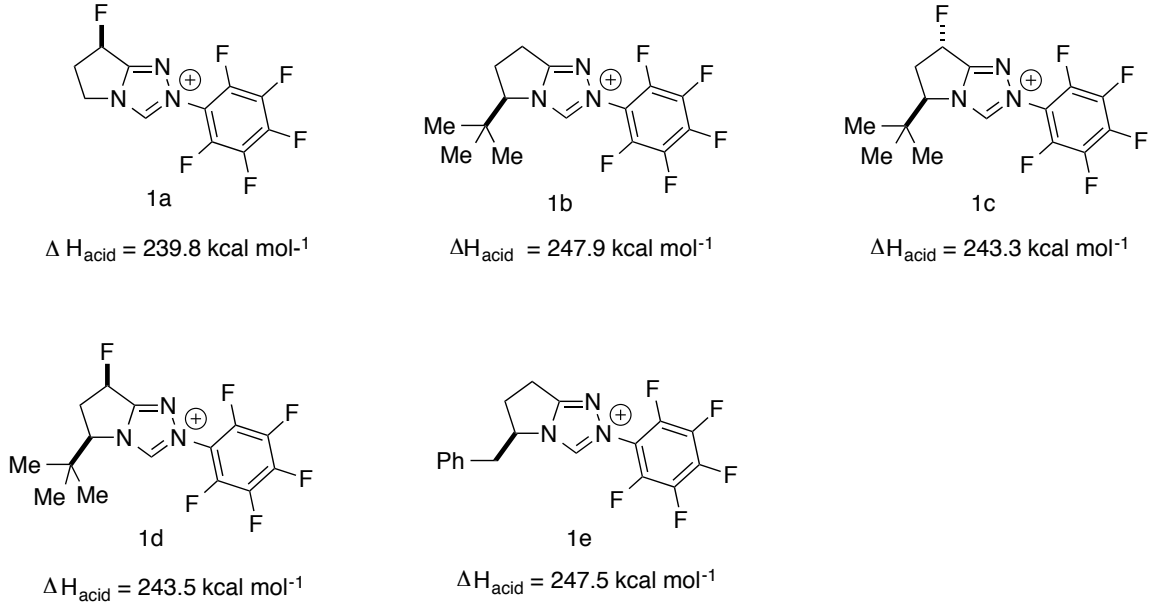

Figure 3. 4 Acidity of morpholine-fused triazolium catalysts by calculation. (ΔH at 298K, B3LYP/6-31+G(d))

The acidity of the protonated pyrrolidine-fused triazolium catalysts is shown in Figure 3.5. As we can see, an electron-donating group at the phenyl ring makes the catalyst more

basic, while an electron-withdrawing group makes the catalyst more acidic.

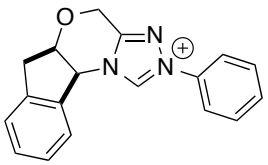

2a

ΔH_{acid} = 252.9 kcal mol^{-1}

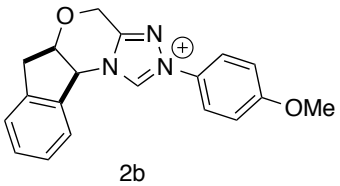

2b

ΔH_{acid} = 256.0 kcal mol^{-1}

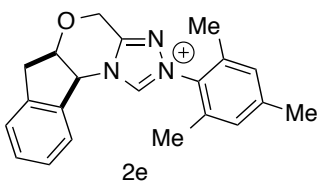

2e

ΔH_{acid} = 257.3 kcal mol^{-1}

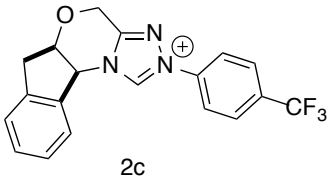

2c

ΔH_{acid} = 246.7 kcal mol^{-1}

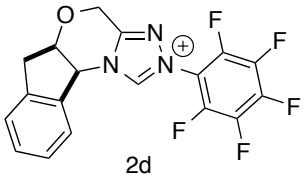

2d

ΔH_{acid} = 244.6 kcal mol^{-1}

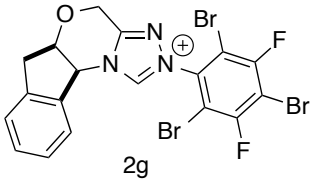

2g

ΔH_{acid} = 247.2 kcal mol^{-1}

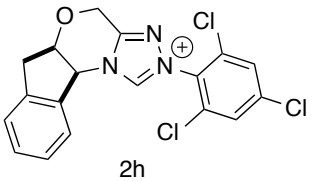

2h

ΔH_{acid} = 249.8 kcal mol^{-1}

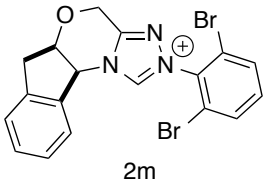

2m

ΔH_{acid} = 252.8 kcal mol^{-1}

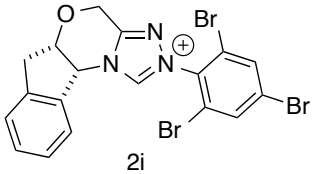

2i

ΔH_{acid} = 251.1 kcal mol^{-1}

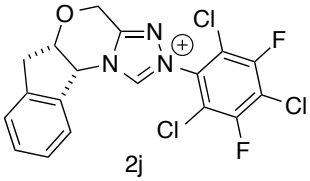

2j

ΔH_{acid} = 246.6 kcal mol^{-1}

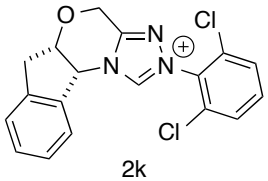

2k

ΔH_{acid} = 252.7 kcal mol^{-1}

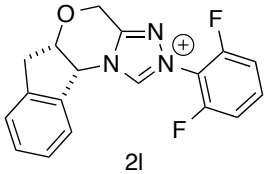

2l

ΔH_{acid} = 251.6 kcal mol^{-1}

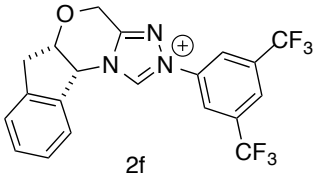

2f

ΔH_{acid} = 241.8 kcal mol^{-1}

Figure 3. 5 Acidity of pyrrolidine-fused triazolium catalysts by calculation. (ΔH at 298K, B3LYP/6-31+G(d))

3.3.2 Bracketing results

In order to benchmark our calculation results, we also conducted the bracketing experiments on a LCQ mass spectrometer. **1a** was allowed to react with several reference bases. The bracketing results are shown in Table 3.1. Proton transfer was not observed when the PA of the reference base was lower than 242.1 kcal/mol, while proton transfer occurs when the PA of the reference base was higher than 243.6 kcal/mol. In this case, we can nail down the PA of the triazolium carbene **1a** to be 243 ± 3 kcal/mol. Compared with the calculation value 239.8 kcal/mol, we think it's consistent.

Table 3. 1 Summary of the PA bracketing result for 1a.

Ref. Compound	Proton Affinity (kcal/mol)[a]	Proton Transfer
Triethylamine	234.7	-
N,N-dimethylcyclohexylamine	235.1	-
Tributylamine	238.6	-
1,4-diaminobutane	240.3	-
N,N,N',N'-Tetramethylethylenediamine	242.1	-
1-Pyrrolidino-1-cyclopentene	243.6	+
N,N,N',N'-tetrametyl-1,3-propanediamine	247.4	+

[a] PAs are in kcal mol^{-1} and were taken from NIST website.

We also conducted bracketing experiments for **1b**, **1c**, **1d** and **1e**. Several reference bases were chosen to react with them respectively; their bracketing results are summarized in Table 3.2.

Table 3. 2 Summary of the PA bracketing results for 1a, 1b, 1c, 1d, 1e.

Trizolium catalyst	Calculation results kcal/mol	Bracketing results kcal/mol
1a	239.8	243 ± 3
1b	247.9	248 ± 3
1c	243.3	248 ± 3
1d	243.5	246 ± 3
1e	247.5	249 ± 3

From Table 3.2, we can see that the calculation results and the bracketing results are consistent for **1a**, **1b**, **1d** and **1e**. However, the bracketed PA value for **1c** is slightly larger than its calculated PA Interestingly, **1c** and **1d** have the same PA by calculation, but **1c** is 2 kcal/mol more basic than **1d**. We predict that the kinetic acidity might play a role causing this difference. In order to support this hypothesis, electrostatic potential maps (ESP) were generated for the gas phase optimized structures of protonated **1c** and **1d** (Figure 3.6). The bulky *t*-Bu group at the back of the triazole ring sterically shields the proton. To avoid hindrance, the base prefers to approach the proton from the front face. For **1d**, the front face has a larger positive charged region (dark blue) than **1c**, which has a superior attraction to the base due to electrostatic interactions. This may explain why **1d** is slightly more basic than **1c**.

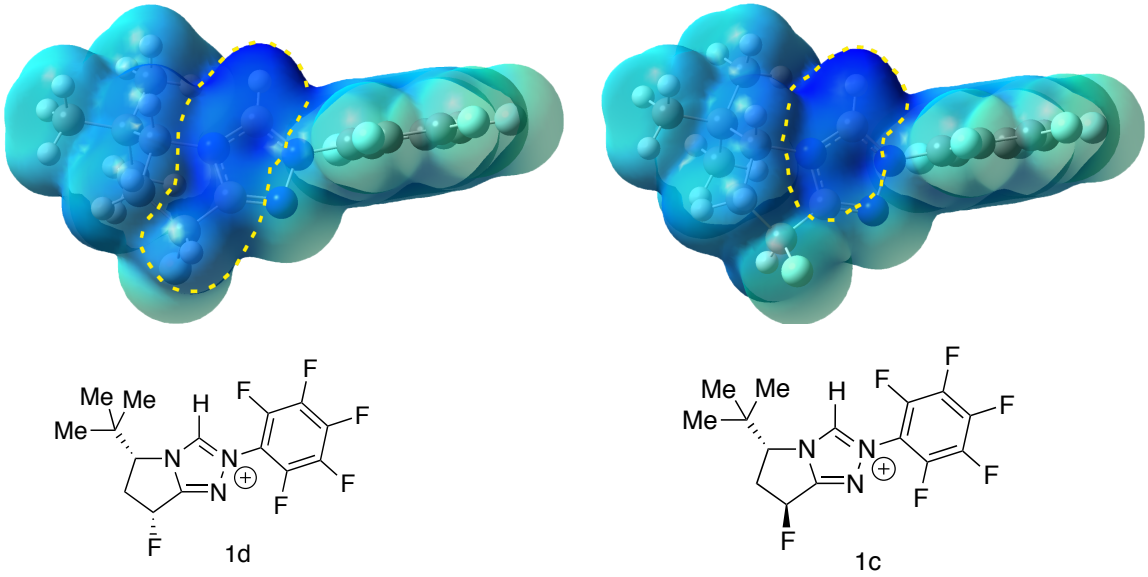

Figure 3. 6 Calculated electrostatic potential surface for 1d and 1c.

3.3.3 Catalytic reactivity of 1c *vs* 1d

Michael acceptor nitroalkene was developed in the intermolecular Stetter reaction by Dr. Rovis (Figure 3.7).[56] Under optimized conditions, catalysts lacking the C_6F_5 *N*-aryl substituent proved inactive. While morpholinyl-based catalyst **6'** was less effective. Triazolium salt **8** generated the desired product in 90% yield and 88% ee. The use of fluorinated triazolium salt **10** under these conditions showed increased reactivity and enantioselectivity as compared to the nonfluorinated analogue **8**, giving the product in 95% yield and 95% ee. However, triazolium salt **11** displayed decreased reactivity with no apparent change in enantioselectivity compared to the nonfluorinated analogue **8**.

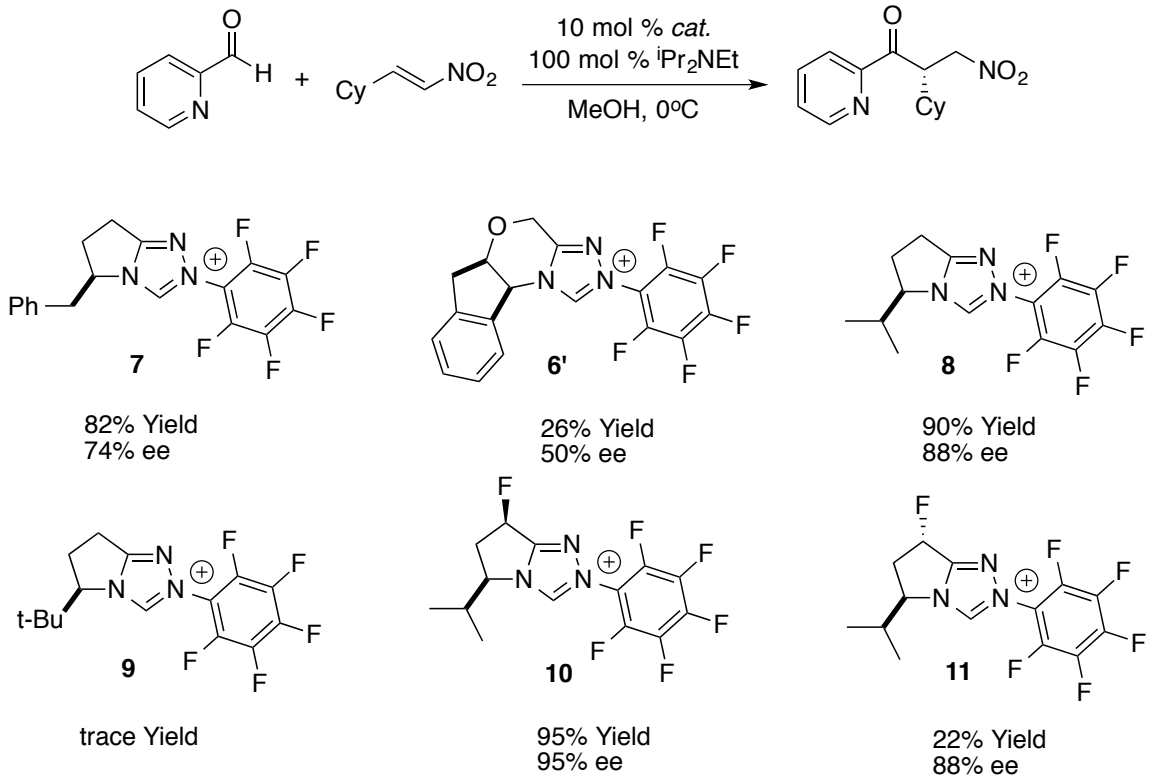

Figure 3. 7 Intermolecular Stetter reaction by Rovis.

However, another intermolecular Stetter reaction developed by Dr. Rovis showed a reverse trend in fluorinated triazolium catalysts (Figure 3.8).[57] By using more reactive Michael acceptor β-nitro-styrenes, pre-catalyst **10**, which previously demonstrated high reactivity and enantioselectivity for hetaryl aldehydes and enals, afforded only modest yields 53% with low enantioselectivity 48%. Surprisingly, *trans*-fluorinated pre-catalyst **11** provided increases in both yield and enantioselectivity, 75% and 74%, respectively. More steric hindered pre-catalyst **1c** gave increased enantioselectivity and yield, 93% and 80%, respectively.

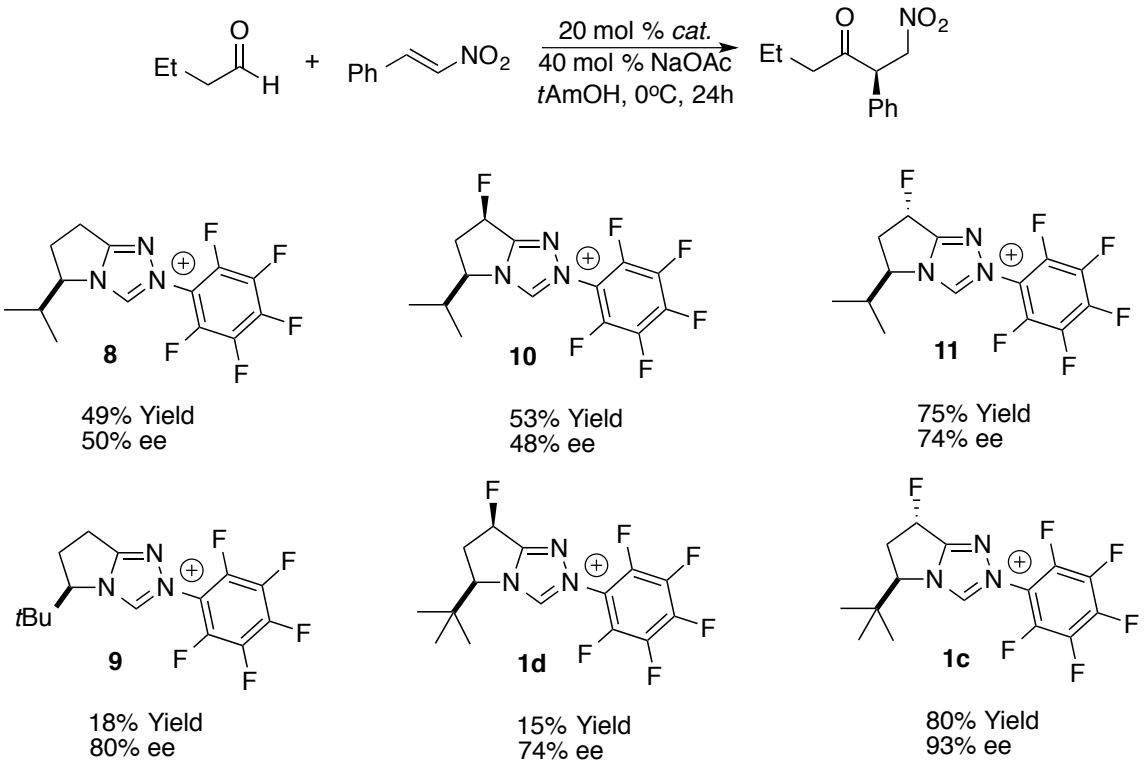

Figure 3. 8 Intermolecular Stetter reaction by Rovis.

Collett and coworkers demonstrated that the overall rate of intramolecular Stetter reaction correlated to the acidity of C(α) proton (Figure 3.9).[58] In order to determine whether C(α) proton plays a role in the reactivity difference of *trans* and *cis* fluorinated triazolium catalyst, acidity calculation for these catalysts were conducted (Figure 3.10). In the gas phase, *cis* fluorinated catalyst **1d** is slightly more acidic than *trans* **1c** by 1 kcal/mol, and this difference is reduced to 0.7 kcal/mol in methanol. For isopropyl triazolium, *cis* fluorinated catalyst **5** is slightly more acidic than the *trans* catalyst **6** by 0.6 kcal/mol, Interestingly, the *cis* catalyst is less acidic than *trans* in methanol by 0.9 kcal/mol. According to the acidity calculation in the gas phase and methanol, we concluded that the acidity of C(α) proton cannot explain the reactivity difference of *trans* and *cis* fluorinated catalyst.

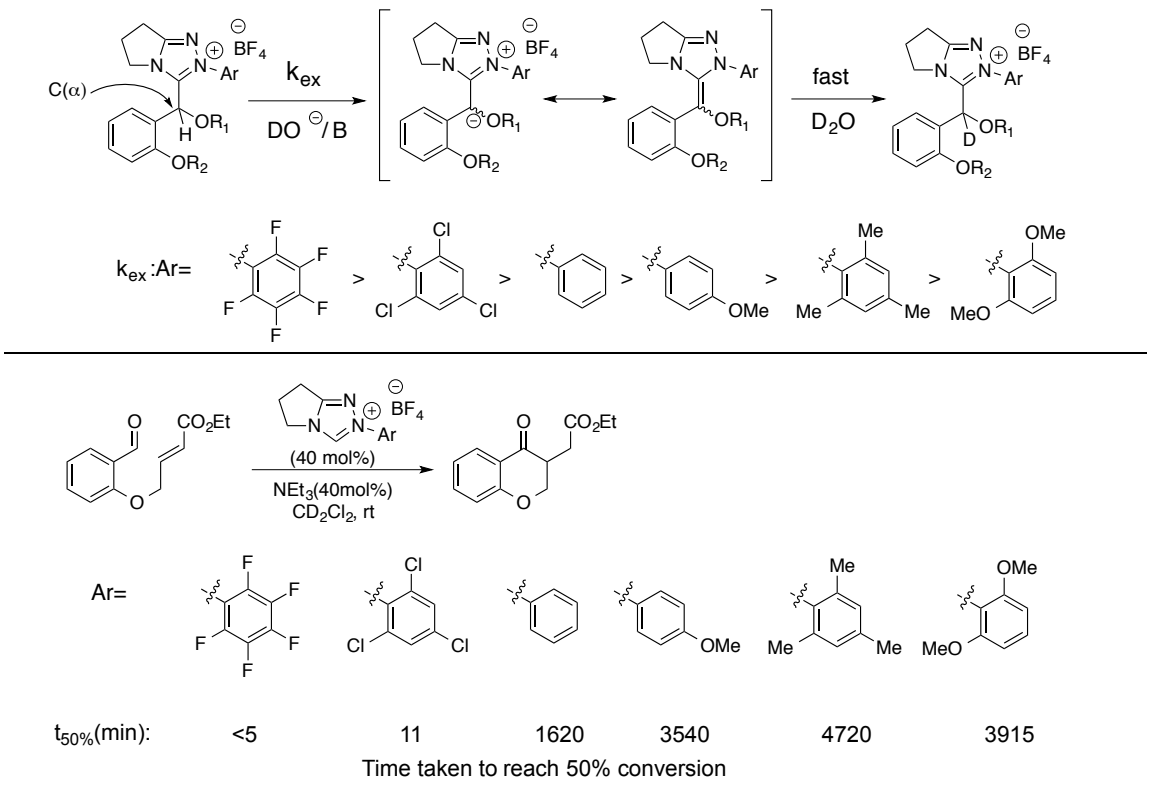

Figure 3. 9 Acidity of C(α) proton and reaction conversion rate.

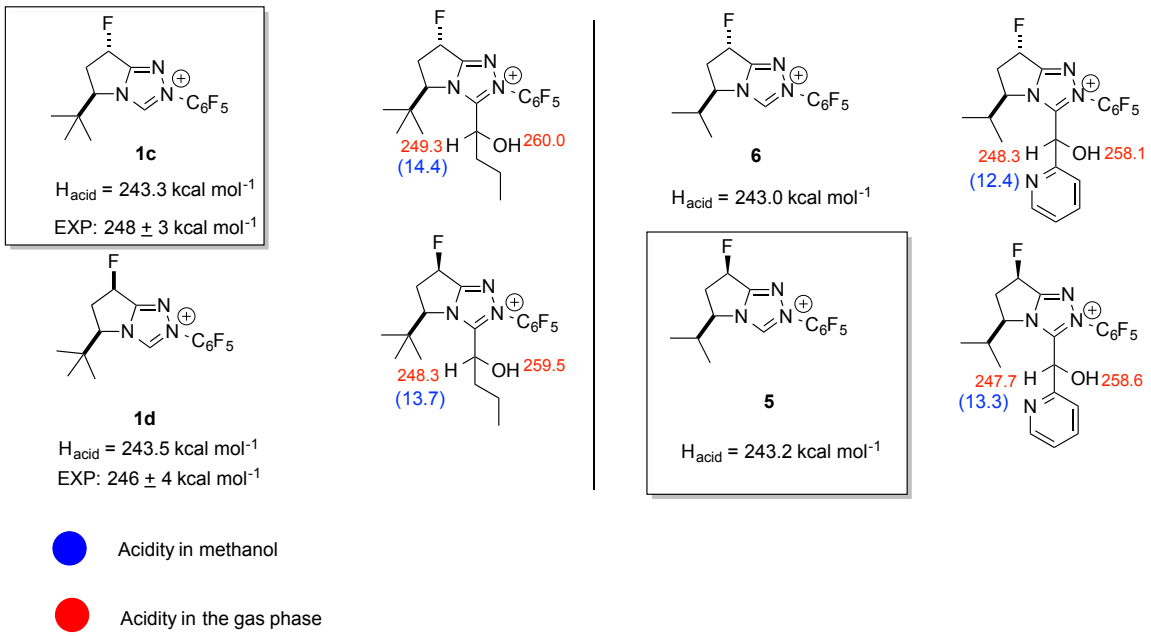

Figure 3. 10 Calculation of acidity in the gas phase and methanol. (ΔH at 298K, B3LYP/6-31+G(d))

To explain why **1c** is superior to **1d** inthe Stetter reaction of aliphatic aldehyde, we hypothesized that the back facing F on **1c** lures the aldehyde in via a dipole-dipole interaction between the fluoro and carbonyl group, enhancing the electrophilicity of the aldehyde. The ion-molecule complex of catalyst+aldehyde was obtained in the gas phase (Figure 3.11). The bond distance between the fluorine and the carbonyl carbon in **1c** is 0.1 Å shorter than in **1d**. On the other hand, formation of the ion-molecular complex is more exothermic for **1c** than for **1d**. This suggests that the dipole-dipole interaction between the fluoro and carbonyl group in **1c** is stronger than in **1d**, making **1c** superior in the Stetter reaction.

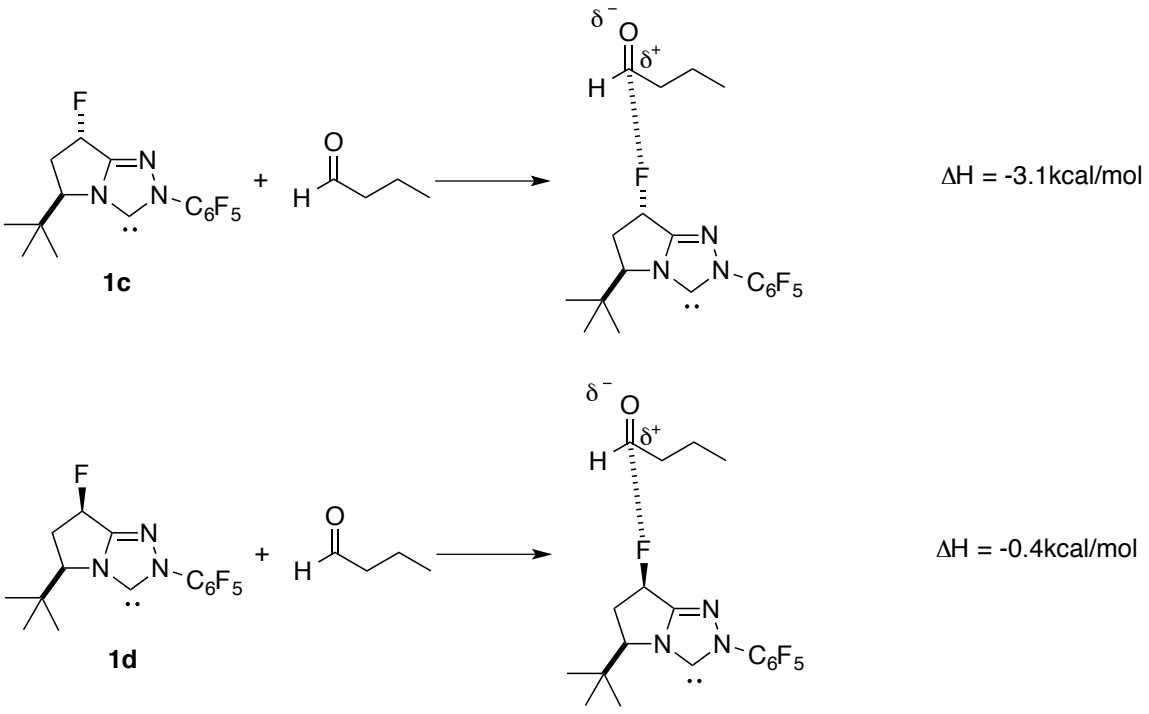

Figure 3. 11 Calculated enthalpy change of forming ion molecular complex.

To explain why **5** is superior than **6** in the aromatic aldehyde involved Stetter reaction, we hypothesized that the electron cloud of the fluoro group repels the aromatic ring of the

aldehyde, due to electrostatic interactions, which inhibits the approach of the aldehyde to the carbene center. For catalyst **5** and **6**, the aldehyde will approach the catalyst from the back face due to the bulky isopropyl group in the front face. The fluorine atom of **6** is located in the back, which further inhibits the approach of the aldehyde from the back. However, the fluorine atom of **5** is located in the front, which will not affect the approach of the aldehyde from the back. This may explain why catalyst **5** is superior than **6** in this reaction.

We also calculated the ion-molecule complex of catalyst+aldehyde in the gas phase (Figure 3.12). To form the ion-molecular complex, *trans* is more exothermic than *cis*. In this way, the *trans* fluorinated complex will inhibit the approach of the second aldehyde to the carbene center and lower the efficiency of the catalyst **6**. This may also explain why **5** is better than **6** in this reaction.

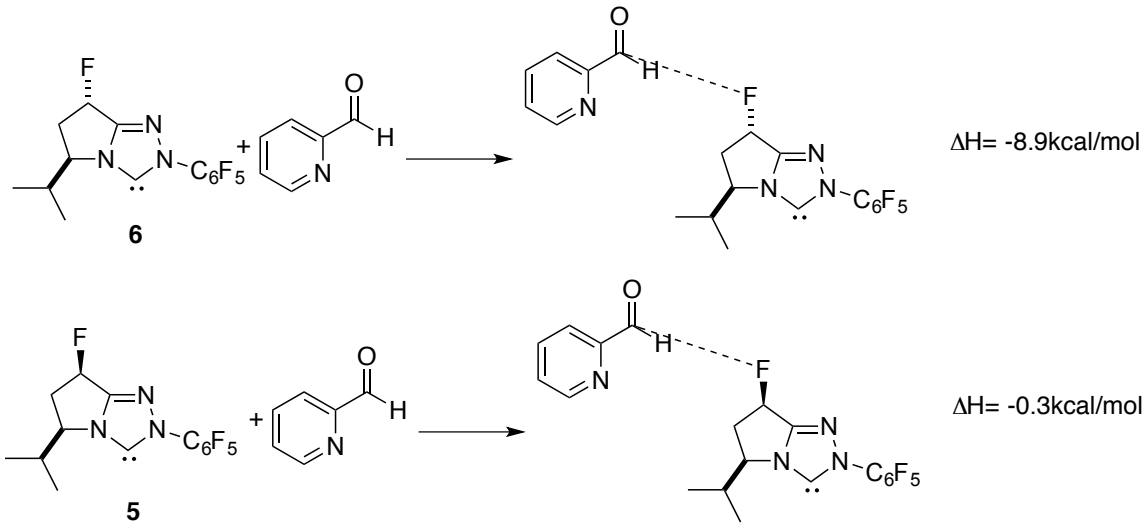

Figure 3.12 Calculated enthalpy change of forming ion molecular complex.

3.4 Conclusion

The acidity of two families of triazolium catalysts, which demonstrated high reactivity in Stetter reaction have been calculated. LCQ bracketing method was used to measure the gas phase acidity of morpholine-fused triazolium catalysts, the experimental results were consistent with the calculation results except for catalysts **1c** and **1d**. Kinetic acidity issue was proposed to explain the discrepancy between the calculation and experiment results. In addition, the hypothesis of a unusual reactivity and selectivity difference for *trans* and *cis* fluorinated catalysts were proposed.

References

(1) Lapworth, A., *J. Chem. Soc., Trans.* **1904,** *85*, 1206-1214.
(2) Breslow, R., *J. Am. Chem. Soc.* **1958,** *80*, 3719-3726.
(3) Chen, Y. T.; Jordan, F., *J. Org. Chem.* **1991,** *56*, 5029-5038.
(4) Breslow, R.; Kim, R., *Tetrahedron Lett.* **1994,** *35*, 699-702.
(5) Breslow, R.; Schmuck, C., *Tetrahedron Lett.* **1996,** *37*, 8241-8242.
(6) Berkessel, A.; Elfert, S.; Yatham, V. R.; Neudörfl, J.-M.; Schlörer, N. E.; Teles, J. H., *Angew. Chem. Int. Ed.* **2012,** *51*, 12370-12374.
(7) Lemal, D. M.; Lovald, R. A.; Kawano, K. I. *J. Am. Chem. Soc.* **1964**, *86*, 2518-2519.
(8) Castells, J.; López-Calahorra, F.; Geijo, F.; Pérez-Dolz, R.; Bassedas, M. *J. Heterocycl. Chem.* **1986**, *23*, 715-720.
(9) Castells, J.; Lopez-Calahorra, F.; Domingo, L., *J. Org. Chem.* **1988,** *53*, 4433-4436.
(10) Castells, J.; Domingo, L.; López-Calahorra, F.; Martí, J., *Tetrahedron Lett.* **1993,** *34*, 517-520.
(11) Martí, J.; Castells, J.; López-Calahorra, F., *Tetrahedron Lett.* **1993,** *34*, 521-524.
(12) López-Calahorra, F.; Rubires, R., *Tetrahedron* **1995,** *51*, 9713-9728.
(13) Martí, J.; López-Calahorra, F.; Bofill, J. M., *J. Mol. Struct. THEOCHEM* **1995,** *339*, 179-194.
(14) López-Calahorra, F.; Castro, E.; Ochoa, A.; Martí, J., *Tetrahedron Lett.* **1996,** *37*, 5019-5022.
(15) Sheehan, J. C.; Hara, T. *J. Org. Chem.* **1974**, *39*, 1196-1199.
(16) Knight, R. L.; Leeper, F. J. *Tetrahedron Lett.* **1997**, *38*, 3611-3614.
(17) Dvorak, C. A.; Rawal, V. H. *Tetrahedron Lett.* **1998**, *39*, 2925-2928.
(18) Isabel Piel, I.; Pawelczyk. D. M.; Hirano Keiichi.; Fröhlich R.; Glorius F. *Eur. J. Org. Chem.* **2011**, 28, 5475-5484.
(19) Santos, L. S.; Pavam, C. H.; Almeida, W. P.; Coelho, F.; Eberlin, M. N., *Angew. Chem. Int. Ed.* **2004,** *43*, 4330-4333.
(20) Marquez, C.; Metzger, J. O., *Chem. Commun.* **2006**, 1539-1541.
(21) Milagre, C. D. F.; Milagre, H. M. S.; Santos, L. S.; Lopes, M. L. A.; Moran, P. J. S.; Eberlin, M. N.; Rodrigues, J. A. R., *J. Mass Spectrom.* **2007,** *42*, 1287-1293.
(22) Schrader, W.; Handayani, P. P.; Burstein, C.; Glorius, F. *Chem. Comm.* **2007**, 716-718.
(23) Lalli, P. M.; Rodrigues, T. S.; Arouca, A. M.; Eberlin, M. N.; Neto, B. A. D., *RSC Advances* **2012,** *2*, 3201-3203.
(24) Seebach, D. *Angew. Chem. Int. Ed.* **1979**, *18*, 239-258.
(25) Stetter, H.; Schreckenberg, M., *Angew. Chem. Int. Ed.* **1973,** *12*, 81-81.

(26) Enders, D.; Breuer, K.; Runsink, J.; Teles, J. H., *Helvetica Chimica Acta* **1996,** *79*, 1899-1902.

(27) Enders, D.; Han, J.; Henseler, A., *Chem. Commun.* **2008,** *0*, 3989-3991.

(28) Kerr, M. S.; Read de Alaniz, J.; Rovis, T., *J. Am. Chem. Soc.* **2002,** *124*, 10298-10299.

(29) Kerr, M. S.; Rovis, T., *J. Am. Chem. Soc.* **2004,** *126*, 8876-8877.

(30) Liu, Q.; Perreault, S. p.; Rovis, T., *J. Am. Chem. Soc.* **2008,** *130*, 14066-14067.

(31) de Alaniz, J. R.; Kerr, M. S.; Moore, J. L.; Rovis, T., *J. Org. Chem.* **2008,** *73*, 2033-2040.

(32) Liu, Q.; Rovis, T., *J. Am. Chem. Soc.* **2006,** *128*, 2552-2553.

(33) DiRocco, D. A.; Oberg, K. M.; Dalton, D. M.; Rovis, T., *J. Am. Chem. Soc.* **2009,** *131*, 10872-10874.

(34) Liu, Q.; Rovis, T., *Org. Lett.* **2009,** *11*, 2856-2859.

(35) DiRocco, D. A.; Rovis, T., *J. Am. Chem. Soc.* **2011,** *133*, 10402-10405.

(36) DiRocco, D. A.; Noey, E. L.; Houk, K. N.; Rovis, T., *Angew. Chem. Int. Ed.* **2012,** *51*, 2391-2394.

(37) Yamashita, M.; Fenn, J. B., *J. Phys. Chem.* **1984,** *88*, 4451-4459.

(38) Fenn, J. B.; Mann, M.; Meng, C. K.; Wong, S. F.; Whitehouse, C. M. *Science* **1989**, *246*, 64-71.

(39) Paul, W.; Steinwedel, H. S. *Naturforsch* **1953**, 8a, 448.

(40) Sharma, S.; Lee, J. K. *J. Org. Chem.* **2002**, 67, 8360-8365.

(41) Liu, M.; Chen, M.; Zhang, S.; Yang, I.; Buckley, B.; Lee, J. K. *J. Phys. Org. Chem.* **2011**, 24, 929-936.

(42) Gaussian 09, Revision A.01, Frisch, M. J.; Trucks, G. W.; Schlegel, H. B.; Scuseria, G. E.; Robb, M. A.; Cheeseman, J. R.; Scalmani, G.; Barone, V.; Mennucci, B.; Petersson, G. A.; Nakatsuji, H.; Caricato, M.; Li, X.; Hratchian, H. P.; Izmaylov, A. F.; Bloino, J.; Zheng, G.; Sonnenberg, J. L.; Hada, M.; Ehara, M.; Toyota, K.; Fukuda, R.; Hasegawa, J.; Ishida, M.; Nakajima, T.; Honda, Y.; Kitao, O.; Nakai, H.; Vreven, T.; Montgomery, Jr., J. A.; Peralta, J. E.; Ogliaro, F.; Bearpark, M.; Heyd, J. J.; Brothers, E.; Kudin, K. N.; Staroverov, V. N.; Kobayashi, R.; Normand, J.; Raghavachari, K.; Rendell, A.; Burant, J. C.; Iyengar, S. S.; Tomasi, J.; Cossi, M.; Rega, N.; Millam, N. J.; Klene, M.; Knox, J. E.; Cross, J. B.; Bakken, V.; Adamo, C.; Jaramillo, J.; Gomperts, R.; Stratmann, R. E.; Yazyev, O.; Austin, A. J.; Cammi, R.; Pomelli, C.; Ochterski, J. W.; Martin, R. L.; Morokuma, K.; Zakrzewski, V. G.; Voth, G. A.; Salvador, P.; Dannenberg, J. J.; Dapprich, S.; Daniels, A. D.; Farkas, Ö.; Foresman, J. B.; Ortiz, J. V.; Cioslowski, J.; Fox, D. J. Gaussian, Inc., Wallingford CT, 2009.

(43) Kohn, W.; Becke, A. D.; Parr, R. G. *J. Phys. Chem.* **1996**, *100*, 12974-12980.

(44) Lee, C.; Yang, W.; Parr, R. G. *Phys. Rev. B* **1988**, *37*, 785-789.
(45) Becke, A. D. *J. Chem. Phys.* **1993**, *98*, 5648-5652.
(46) Becke, A. D. *J. Chem. Phys.* **1993**, *98*, 1372-1377.
(47) Ugai, T.; Tanaka, S.; Dokawa, S., *J. Pharm. Soc. Jpn.* **1943,** *63*, 269-300.
(48) Krampitz, L. O.; Greull, G.; Miller, C. S.; Bicking, H. R.; Skeggs, H. R.; Sprague, J. M. *J. Am. Chem. Soc.* **1958**, 80, 5893-5894.
(49) Berkessel, A.; Elfert, S.; Etzenbach-Effers, K.; Teles, J. H., *Angew. Chem. Int. Ed.* **2010,** *49*, 7120-7124.
(50) Marenich, A. V.; Cramer, C. J.; Truhlar, D. G. *J. Phys. Chem. B* **2009**, *113*, 6378–6396.
(51) Miertuš, S.; Scrocco, E.; Tomasi, J. *Chem. Phys.* **1981**, *55*, 117–129.
(52) Pascual-Ahuir, J. L.; Silla, E.; Tuñón, I. *J. Comput. Chem.* **1994**, *15*, 1127–1138.
(53) Stetter, H.; Raemsch, R. Y.; Kuhlmann, H. *Synthesis* **1976**, 733-735.
(54) Ciganek, E. *Synthesis* **1995**, 1311-1314.
(55) Rovis, T. *Chem. Lett.* **2008**, *37*, 2-7.
(56) DiRocco, D. A.; Oberg, K. M.; Dalton, D. M.; Rovis, T., *J. Am. Chem. Soc.* **2009,** *131*, 10872-10874.
(57) DiRocco, D. A.; Noey, E. L.; Houk, K. N.; Rovis, T., *Angew. Chem. Int. Ed.* **2012,** *51*, 2391-2394.
(58) Collett, C. J.; Massey, R. S.; Maguire, O. R.; Batsanov, A. S.; O'Donoghue, A. C.; Smith, A. D., *Chem. Sci.* **2013,** *4*, 1514-1522.